



Minerva Access is the Institutional Repository of The University of Melbourne

Author/s:

Shepherd, RK;Carter, PM;Dalrymple, AN;Enke, YL;Wise, AK;Nguyen, T;Firth, J;Thompson, A;Fallon, JB

Title:

Platinum dissolution and tissue response following long-term electrical stimulation at high charge densities

Date:

2021-06-01

Citation:

Shepherd, R. K., Carter, P. M., Dalrymple, A. N., Enke, Y. L., Wise, A. K., Nguyen, T., Firth, J., Thompson, A. & Fallon, J. B. (2021). Platinum dissolution and tissue response following long-term electrical stimulation at high charge densities. *Journal of Neural Engineering*, 18 (3), <https://doi.org/10.1088/1741-2552/abe5ba>.

Persistent Link:

<https://hdl.handle.net/11343/307907>

License:

CC BY

PAPER • OPEN ACCESS

# Platinum dissolution and tissue response following long-term electrical stimulation at high charge densities

To cite this article: Robert K Shepherd *et al* 2021 *J. Neural Eng.* **18** 036021

View the [article online](#) for updates and enhancements.

You may also like

- [Evaluation of focused multipolar stimulation for cochlear implants: a preclinical safety study](#)  
Robert K Shepherd, Andrew K Wise, Ya Lang Enke et al.
- [Electrochemical and biological characterization of thin-film platinum-iridium alloy electrode coatings: a chronic \*in vivo\* study](#)  
Ashley N Dalrymple, Mario Huynh, Bryony A Nayagam et al.
- [Drug delivery to the inner ear](#)  
Andrew K Wise and Lisa N Gillespie



## PAPER

## OPEN ACCESS

## RECEIVED

30 September 2020

## REVISED

11 January 2021

## ACCEPTED FOR PUBLICATION

12 February 2021

## PUBLISHED

17 March 2021

Original content from this work may be used under the terms of the [Creative Commons Attribution 4.0 licence](#).

Any further distribution of this work must maintain attribution to the author(s) and the title of the work, journal citation and DOI.



# Platinum dissolution and tissue response following long-term electrical stimulation at high charge densities

Robert K Shepherd<sup>1,2,\*</sup> , Paul M Carter<sup>3</sup> , Ashley N Dalrymple<sup>1,4</sup> , Ya Lang Enke<sup>3</sup> , Andrew K Wise<sup>1,2</sup> , Trung Nguyen<sup>1</sup>, James Firth<sup>1</sup>, Alex Thompson<sup>1</sup>  and James B Fallon<sup>1,2</sup> 

<sup>1</sup> Bionics Institute, St Vincent's Hospital, Melbourne, Australia

<sup>2</sup> Medical Bionics Department, University of Melbourne, Melbourne, Australia

<sup>3</sup> Cochlear Ltd, Sydney, Australia

<sup>4</sup> Department of Mechanical Engineering, Carnegie Mellon University, Pittsburgh, PA, United States of America

\* Author to whom any correspondence should be addressed.

E-mail: [rshepherd@bionicsinstitute.org](mailto:rshepherd@bionicsinstitute.org)

**Keywords:** electrical stimulation, neural prosthesis, platinum, electrode, stimulation safety, corrosion, cochlear implant, neurotechnology

Supplementary material for this article is available [online](#)

## Abstract

**Objective.** Established guidelines for safe levels of electrical stimulation for neural prostheses are based on a limited range of the stimulus parameters used clinically. Recent studies have reported particulate platinum (Pt) associated with long-term clinical use of these devices, highlighting the need for more carefully defined safety limits. We previously reported no adverse effects of Pt corrosion products in the cochleae of guinea pigs following 4 weeks of electrical stimulation using charge densities far greater than the published safe limits for cochlear implants. The present study examines the histopathological effects of Pt within the cochlea following continuous stimulation at a charge density well above the defined safe limits for periods up to 6 months. **Approach.** Six cats were bilaterally implanted with Pt electrode arrays and unilaterally stimulated using charge balanced current pulses at a charge density of  $267 \mu\text{C cm}^{-2} \text{ phase}^{-1}$  using a tripolar electrode configuration. Electrochemical measurements were made throughout the implant duration and evoked potentials recorded at the outset and on completion of the stimulation program. Cochleae were examined histologically for particulate Pt, tissue response, and auditory nerve survival; electrodes were examined for surface corrosion; and cochlea, brain, kidney, and liver tissue analysed for trace levels of Pt. **Main results.** Chronic stimulation resulted in both a significant increase in tissue response and particulate Pt within the tissue capsule surrounding the electrode array compared with implanted, unstimulated control cochleae. Importantly, there was no stimulus-induced loss of auditory neurons (ANs) or increase in evoked potential thresholds. Stimulated electrodes were significantly more corroded compared with unstimulated electrodes. Trace analysis revealed Pt in both stimulated and control cochleae although significantly greater levels were detected within stimulated cochleae. There was no evidence of Pt in brain or liver; however, trace levels of Pt were recorded in the kidneys of two animals. Finally, increased charge storage capacity and charge injection limit reflected the more extensive electrode corrosion associated with stimulated electrodes. **Significance.** Long-term electrical stimulation of Pt electrodes at a charge density well above existing safety limits and nearly an order of magnitude higher than levels used clinically, does not adversely affect the AN population or reduce neural function, despite a stimulus-induced tissue response and the accumulation of Pt corrosion product. The mechanism resulting in Pt within the unstimulated cochlea is unclear, while the level of Pt observed systemically following stimulation at these very high charge densities does not appear to be of clinical significance.

## 1. Introduction

Platinum (Pt) is regarded as a safe electrode material when used in combination with carefully controlled charge-balanced current pulses operating within stimulus levels that allow charge injection via reversible Faradaic reactions [1, 2]. However, high charge intensities can generate irreversible electrochemical reactions including the hydrolysis of water, Pt dissolution and O<sub>2</sub> reduction, altering the electrolyte environment adjacent to the electrode that may result in both electrode corrosion and tissue damage [2–6].

There are useful guidelines defining the boundary between damaging and non-damaging electrical stimulation for neural prostheses using Pt electrodes. The ‘Shannon limit’ [7] was generated from acute stimulation studies using large surface area Pt electrodes in direct contact with cortical neurons and typically stimulated at 50 pulses per second (pps) for ~8 h [8]. This limit defines the maximum safe relationship between charge density and charge per phase for neural prostheses given by the equation:  $\log(Q/A) = k - \log(Q)$ ; where  $Q$  is the charge per phase ( $\mu\text{C}$  per phase),  $A$  is the geometric surface area of the stimulating electrode ( $\text{cm}^2$ ),  $Q/A$  is the charge density per phase ( $\mu\text{C cm}^{-2} \text{ phase}^{-1}$ ), and the variable  $k$  within the range 1.5–1.85 [1, 2, 7]. However, the stimulus parameters used to derive this relationship represent a subset of the parameters used by neural stimulators operating in a clinical setting [9]. Important parameters, including stimulus rate, near- versus far-field electrodes, duty cycle, electrode material and the target neural population, will influence the boundary between safe and damaging electrical stimulation [1, 9, 10]. In addition to the general guidelines provided by the Shannon limit, the Association for the Advancement of Medical Instrumentation (AAMI) developed a standard for commercial cochlear implants that limits stimulation to a Shannon limit of  $k = 1.75$ , with a maximum charge density of  $216 \mu\text{C cm}^{-2} \text{ phase}^{-1}$  [11].

The need for more carefully defined safe stimulation limits specifically for cochlear implants was highlighted by a series of clinical studies showing evidence of particulate Pt within the tissue capsule surrounding the electrode array in the cochleae of patients that were long-term cochlear implant users [12–15]. Some of these reports also described an increased foreign body response within the cochlea associated with the particulate Pt [14, 15]. Little is known about the toxicity to cochlear tissue, or the systemic distribution of these corrosion products *in vivo*.

Using a deafened guinea pig model of cochlear implantation, we recently demonstrated that chronic stimulation using stimulus parameters as high as  $k = 2.0$ —well above the published guidelines—did not result in loss of primary auditory neurons (ANs) [16, 17]. However, stimulation at these high charge densities did produce significant levels of particulate

Pt within the tissue capsule surrounding the electrode array [16, 17]. Although the extent of the foreign body response was also associated with stimulation at high charge densities, these studies concluded that there were no adverse histopathological effects of Pt corrosion product on tissue within deafened cochleae.

These previous studies were undertaken using continuous stimulation for 4 weeks. The present study extends this work by using a deaf feline model where both cochleae were implanted, and the animals unilaterally stimulated using a tripolar electrode configuration at a charge density of  $267 \mu\text{C cm}^{-2} \text{ phase}^{-1}$  ( $k = 1.73$ ) for periods of up to 6 months. These stimulus parameters were selected as they are above the maximum AAMI standard for cochlear implants [11], and are known to result in significant corrosion of Pt electrodes [16] while being well tolerated in an awake, chronically stimulated animal. We show that long-term stimulation of Pt electrodes at a charge density well above the accepted safety limits induces a vigorous tissue response and Pt corrosion within the cochlea, and extensive corrosion of the surface of stimulated electrodes. Increased charge storage capacity (CSC) and charge injection limit (CIL) was associated with stimulated electrodes. Despite these changes, there was no evidence of a reduction in AN density or evoked-potential threshold associated with the stimulation. Finally, we report trace levels of Pt in implanted, unstimulated control cochleae and in the kidney of chronically stimulated animals. The clinical implications of these findings are discussed.

## 2. Methods

### 2.1. Experimental subjects

This study was performed using a total of six male cats. All procedures were conducted with approval from the Bionics Institute Animal Research and Ethics Committee, and were performed in accordance with the Australian Code of Practice for the Care and Use of Animals for Scientific Purposes (8th Edition, 2013) and followed the principles of the US National Institutes of Health guidelines regarding the care and use of animals for experimental procedures.

### 2.2. Deafening protocol

Animals were deafened as neonates using daily subcutaneous injection of neomycin (neomycin trisulphate;  $60 \text{ mg kg}^{-1}$ ; subcutaneously [s.c.]) [18, 19]. After 3 weeks of deafening each animal was anaesthetised with 3%–4% isoflurane and  $500 \text{ ml min}^{-1}$  oxygen, and maintained at 1%–2% isoflurane. Hearing status was examined by recording the auditory brainstem response (ABR). ABRs were recorded differentially using subcutaneous electrodes (vertex positive; neck negative and thorax ground) and responses amplified, filtered, averaged, and displayed. If there

was evidence of hearing in response to a 100  $\mu$ s duration acoustic click at 100 dB peak-equivalent sound pressure level (p.e. SPL), the neomycin injections were continued until no ABR response at this intensity was evident.

### 2.3. Scala tympani electrode array

HL14 electrode arrays (Cochlear Ltd, Australia) were used in the present study [20]. Each array contained 14 half-band Pt electrodes on a polydimethylsiloxane (PDMS) silicone carrier. Each electrode had a surface area of 0.075 mm<sup>2</sup>. Electrode 1 (E1) was the most basal and electrode 14 (E14) the most apical electrode on the array [21]. Each Pt electrode was connected via a leadwire to a battery powered stimulator (details below) located in a backpack.

### 2.4. Cochlear implant surgery

Animals were bilaterally implanted at 8 weeks of age using aseptic surgical techniques. Each animal was pre-medicated with an intramuscular injection of Ketamine (10 mg kg<sup>-1</sup>) and Xylazine (1 mg kg<sup>-1</sup>), and anaesthesia was maintained at a surgical level using a closed circuit anaesthetic machine (1%–2% isoflurane and 500 ml min<sup>-1</sup> oxygen). The bulla cavity was opened, the round window incised and the electrode array was inserted into the scala tympani to the lower middle turn [20]. The round window was sealed with crushed muscle to prevent perilymph leakage. The leadwire was fixed at the bulla and on the skull, and then passed subcutaneously to exit the body through an incision over the scapula. During surgery, the animal's respiratory rate, expired CO<sub>2</sub>, and body temperature were monitored and maintained within normal levels (respiration rate 15–30; expired CO<sub>2</sub> 3%–5%; body temperature 37 ± 1 °C). An electrolyte solution (Hartmann's solution, 5–10 ml kg<sup>-1</sup> h<sup>-1</sup>, i.v.) and analgesic (Temgesic, 0.01 mg kg<sup>-1</sup>, s.c.) were administered and a single carprofen injection (4 mg kg<sup>-1</sup> s.c.) administered immediately post-operatively to provide 24 h of mild analgesia. Antibiotics (Clavulox 7 mg kg<sup>-1</sup>, s.c.) were administered on the day of surgery then orally (25 mg kg<sup>-1</sup>) for up to 21 d following surgery.

### 2.5. Electrode impedance

Common ground electrode impedances measured between the electrode of interest and the remaining electrodes on the cochlear array were recorded at least weekly in awake animals using Custom Sound EP 5.1 (Cochlear, Ltd, Australia). Because recent stimulation history can influence electrode impedance [22], these measurements were made immediately following disconnection from the stimulator. If any electrode had an impedance value greater than 20 k $\Omega$ , the electrode was considered open circuit and was no longer used for stimulation. This prompted a change in the stimulation electrode configuration from a tripolar to a bipolar configuration. However, analysis

of common ground impedances included electrodes with an impedance greater than 20 k $\Omega$  but less than 50 k $\Omega$ .

### 2.6. *In vivo* electrochemical measurements

Electrochemical measurements were conducted on both the stimulated and the unstimulated control electrode arrays. Electrochemical impedance spectroscopy (EIS), cyclic voltammetry (CV), and CIL were recorded using the tripolar or bipolar configuration based on electrode availability (see below), as a standard three-electrode cell recording configuration was not feasible *in vivo*. The centre-electrode of the tripole or dipole was used as the working electrode; for tripolar recordings, the flanking-electrodes were used as the counter electrode, and the reference electrode was an unstimulated electrode on the array; for bipolar recordings, the flanker-electrode was used as the counter and reference electrodes combined.

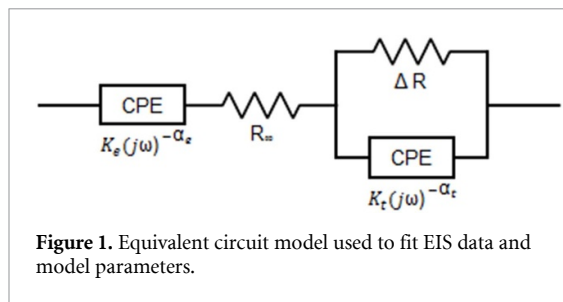
The electrochemical measurements were made under general anaesthesia at three time points post-implant: 2 weeks (i.e. before commencement of the chronic stimulation program), 3 months, and 6 months. The impedance measurements were made immediately following disconnection from the stimulator, and the sequence and duration of the electrochemical recordings were kept constant at each time point to minimize variability due to the effects of stimulation history as noted above ((a) common ground impedances (~5 min, immediately after turning the stimulation off); (b) electrophysiological recordings (~50 min); (c) EIS then CV for each configuration (~45 min); and (d) CIL (~10 min)).

EIS was measured using a potentiostat (Interface 1000E, Gamry Instruments, USA). The frequency values ranged from 100 to 100 000 Hz at 10 points/decade and an AC voltage of 50 mV RMS. The low frequency value was chosen to be 100 Hz to avoid the possibility of DC-induced tissue damage that may occur at lower frequencies [23]. However, at 6 months post-implant, the low frequency value was extended to 1 Hz since this recording was immediately preceding termination.

EIS data were fitted to an equivalent circuit model to quantify the factors influencing the electrode impedance throughout the chronic stimulation program [24, 25]. A common phase element (CPE) was used to represent the capacitive behavior of the impedance at the electrode–electrolyte interface according to the following equation:

$$Z_{\text{CPE}} = \frac{K}{(j\omega)^\alpha} \quad (1)$$

where  $K$  is the magnitude scaling factor,  $\omega$  is the frequency, and  $0 < \alpha < 1$ ; where  $\alpha = 0$  indicates more resistive behavior and  $\alpha = 1$  indicates more capacitive behavior (figure 1) [25–27]. The impedance of the tissue layer is represented by a modified Lapicque equivalent circuit model, which includes the



resistance of the tissue layer at an infinite stimulation frequency ( $R_\infty$ ) in series with a parallel combination of a second CPE representing the tissue capacitance and  $\Delta R$ , where  $\Delta R = (R_0 - R_\infty)$  and  $R_0$  is the resistance of the tissue layer at DC.

CV measurements were performed using the same potentiostat that was used for EIS. The electrode potential cycled between the limits of  $-0.6$  and  $0.8$  V with respect to the counter electrode at a sweep rate of  $150 \text{ mV s}^{-1}$  for five cycles. The CSC was computed from the CV curves by first finding the average of cycles 2 through 5, then integrating the total area of the current over time and dividing by the electrode geometric surface area.

Finally, voltage transient waveforms were measured and used to compute the CIL of each electrode (USB-6353, National Instruments, USA). The CIL was calculated by analysing the voltage response to a series of biphasic, cathodic first current pulses, with a pulse width of  $100 \mu\text{s}$  and current amplitudes ranging from  $50 \mu\text{A}$  to  $2 \text{ mA}$  in steps of  $50 \mu\text{A}$ . The maximum cathodal voltage ( $E_{mc}$ ) was determined by subtracting the access voltage ( $V_a$ ) from the maximum negative potential using a custom algorithm in Igor Version 8.04 (WaveMetrics, Portland, OR, USA). The CIL was calculated using the current value just below the amplitude level that caused the  $E_{mc}$  to surpass the cathodal limit of the water window ( $-0.6 \text{ V}$ ), up to a maximum of  $2 \text{ mA}$  [6, 28].

## 2.7 Electrically-evoked responses

Electrically-evoked auditory nerve compound action potentials (ECAPs) were used to monitor AN function. ECAPs were recorded in awake animals at both the onset of stimulation and at termination using neural response telemetry and Custom Sound EP 2.0 software (Cochlear Ltd, Australia) [21]. ECAP recordings were obtained from electrodes on both the chronically stimulated and control electrode arrays using  $25 \mu\text{s}/\text{phase}$  biphasic pulses at  $80 \text{ pulses s}^{-1}$  in a monopolar electrode configuration. Recordings were made from below threshold to a maximum of  $1600 \mu\text{A}$  or the highest level that did not produce an aversive response using small intensity steps ( $25\text{--}50 \mu\text{A}$ ). ECAP threshold was defined as the lowest current amplitude required to evoke a clear ECAP with an amplitude of at least  $20 \mu\text{V}$ . Thresholds from each chronically stimulated cochlea were compared

statistically with responses recorded from the contralateral implanted/deafened control cochlea.

## 2.8. Chronic stimulation program

One cochlea in each animal was randomly selected to be chronically stimulated while the contralateral cochlea was unstimulated and therefore served as a control. Animals were stimulated continuously ( $24 \text{ h d}^{-1}$ ,  $7 \text{ d per week}$ ) over an implantation period of up to 6 months (table 1).

The chronic stimulation program commenced 2 weeks following implant surgery immediately after recording the initial electrochemical measures under anaesthesia. Each animal was stimulated via a custom built back-pack stimulator [29] that delivered  $2 \text{ mA}$ ,  $100 \mu\text{s phase}^{-1}$  charge balanced biphasic current pulses at  $200 \text{ pps}$ , developing  $0.2 \mu\text{C phase}^{-1}$ . A tripolar electrode configuration was used as it allowed high charge levels to be used while maintaining the percept within the animals' comfortable loudness range [16]. A cathodic first phase current was delivered on the centre-electrode of the tripole while the two flanker-electrodes provided the return path. All currents were then reversed in the second phase of the pulse. Charge-balance was achieved by shorting all electrodes between current pulses [30]; a technique we used previously in a shorter duration study [16]. Multiple (typically four) tripolar sites were stimulated across the 14 electrodes on the array (table 1). Centre tripole electrodes generated charge densities of  $267 \mu\text{C cm}^{-2} \text{ phase}^{-1}$  while the flanker-electrodes developed approximately half this charge density. This stimulus regime was used as we had previously demonstrated significant levels of Pt corrosion at this level [16]. In cases where stimulation using a tripolar configuration was not possible, the stimulating electrodes were reconfigured to bipolar electrodes and maintained the same charge density as in the tripolar configuration. Although the majority of the electrodes on a stimulated array underwent chronic stimulation there were always a number of electrodes that were not subject to stimulation (typically E1 & E2).

## 2.9. Histology

On completion of the stimulation program all animals were euthanized with sodium pentobarbitone ( $300 \text{ mg kg}^{-1}$ ; intraperitoneal) and systemically perfused with heparinised normal saline at  $37^\circ\text{C}$  followed by  $10\%$  neutral buffered formalin at  $4^\circ\text{C}$ . Each electrode array was removed for examination under a scanning electron microscope (SEM; see below) and both the stimulated and contralateral control cochlea postfixed, decalcified, frozen and sectioned at  $12 \mu\text{m}$  to the mid-point using a CM 1900 UV cryostat (Leica, Germany) at  $-22^\circ\text{C}$ . The section plane used is illustrated in figure 2. The remaining half of the cochlea was kept for trace analysis of Pt using inductively

**Table 1.** Summary of the cohorts used in this study.

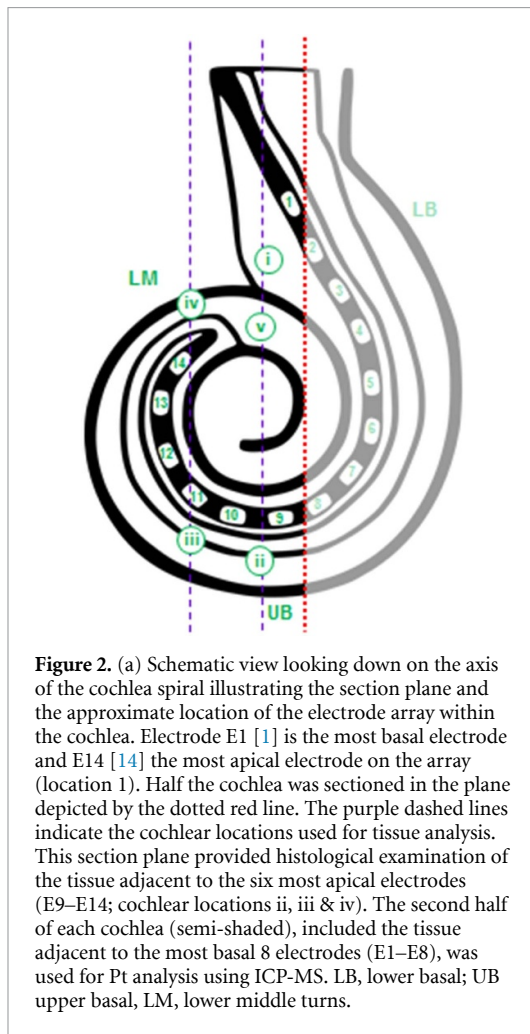
Animal ID	Duration of stimulation (weeks)	Centre-electrode <sup>a</sup> charge density ( $\mu\text{C cm}^{-2} \text{ phase}^{-1}$ )	Stimulated side	Centre-electrodes for each tripole <sup>b</sup>
HCD_1 <sup>c</sup>	7	267	Right	TP4; TP7; TP10; TP13
HCD_2	24	267	Right	TP3; TP6, TP9; TP12
HCD_3	24	267	Left	TP4; TP7; TP10; TP13
HCD_4	24	267	Right	TP4; TP7; TP10; TP13
HCD_5	24	267	Left	TP3; TP6; TP9; TP12
HCD_6	26	267	Right	TP4; TP7; TP10; TP13

Notes:

<sup>a</sup> Throughout this publication charge density refers to that on the centre-electrode of the tripole unless otherwise stated.

<sup>b</sup> In cases where stimulation using a tripolar configuration was not possible, the stimulating electrodes were reconfigured to bipolar electrodes. TP = tripole electrode.

<sup>c</sup> Stimulation program terminated early due to leadwire damage. No terminal impedance, electrochemical recordings or ECAPs were made with this animal.



coupled plasma mass spectrometry (ICP-MS [16]; see below).

A representative series of cochlear sections were stained with haematoxylin and eosin (H&E) for qualitative examination [31]. AN density, and the tissue response within the scala tympani, were quantified and compared statistically with data from the contralateral implanted unstimulated control cochlea. ANs were quantified in mid-modiolar sections using a Zeiss Axioplan microscope by a single

observer blinded to the experimental cohorts. ANs were identified within Rosenthal's canal and counted within the lower basal (LB), upper basal (UB), lower middle (LM), upper middle (UM) and the apical (A) cochlear regions [16, 31]. Only ANs exhibiting a clear nucleus were counted. The area of Rosenthal's canal was measured using Image J software (version 1.52p) and the density of the ANs was determined. The AN density for each cochlear region was averaged from five sections that were spaced at least  $72 \mu\text{m}$  apart, ensuring that no AN was counted more than once.

In order to quantify the tissue response, the extent of fibrosis in the cochlea was measured in H&E stained sections at five locations along the electrode array (locations i–v; figure 2). An image of the scala tympani was captured and its area measured. The 'Triangle' algorithm in Image J was used to automatically threshold the image to quantify the tissue response [31]. The area of scala tympani excluding the area of the electrode array was measured and the proportion of the scala tympani occupied by the tissue response calculated.

In addition to quantifying the extent of the foreign body response, the extent of any focal macrophage response associated with the electrode-tissue capsule was assessed by measuring its thickness in the section of each cochlea displaying the most extensive response [17]. Histological images were digitized using a Zeiss AxioLab microscope and the zone thickness measured using Image J software [16].

All cochleae were examined for evidence of electrode insertion trauma. Histological sections were examined under a microscope by a researcher experienced in cochlear histopathology. Insertion trauma was identified by fracture of the osseous spiral lamina and/or tears to the basilar membrane or the outer cochlear wall. This form of trauma evokes a clear histopathological signature localized to the site of trauma, including a vigorous tissue response, neo-osseogenesis, loss of ANs, and an increased acute inflammatory response.

Each cochlea was also examined histologically for the presence of particulate material [16]. The extent

of this material was qualitatively graded from 0 to 4 (0, no evidence of particulate material in any section; 1 possible particulate material present; 2, clear localised particulate material present; 3, particulate material present in a number of sections; 4, widespread particulate material present).

### 2.10. SEM

Following removal from the cochlea, each electrode array was rinsed, ultrasonically cleaned in distilled water then stored in 70% ethanol. A small number of electrode arrays required additional cleaning in Enzol (diluted 1:40 for 1 h at room temperature; WPI Inc., USA) to remove coatings that had formed over the electrode surface. All electrodes from both stimulated and control electrode arrays were examined using a FEI QUANTA 200 SEM, photographed at low ( $\times 600$ ) and medium ( $\times 2000$ ) magnification. A region of each electrode surface was then randomly selected and photographed at higher magnifications ( $\times 4000$  and  $\times 10\,000$ ). The surface condition of each electrode was evaluated by an experienced investigator blinded to the experimental groups. The severity of Pt corrosion was graded from 0 to 5 (0, no corrosion; 1, no evidence of corrosion but electrode at least partially coated with organic material; 2, localized minor corrosion; 3, localized moderate corrosion; 4, widespread corrosion; 5, severe and extensive corrosion) [16, 21, 32].

Representative unstained cochlear sections from both chronically stimulated and implanted, unstimulated control cochleae were examined under the SEM to identify particulate matter observed within the fibrous tissue capsule of some cochleae. Specific sites associated with the tissue capsule were selected for elemental analysis using an INCA X-Act SDD EDS system with an Oxford Aztec Microanalysis System (3.1). Regions of the fibrous tissue capsule containing the particulate material were compared with regions only containing fibrous tissue [16].

### 2.11. Trace analysis of Pt

The un-sectioned half of each cochlea covering the region occupied by electrodes E1–E8 (figure 1) was measured for Pt using ICP-MS by the National Measurement Institute of the Australian Government [16]. Both the chronically stimulated and the contralateral (control) cochleae were examined for trace Pt using this technique. In addition to the cochleae, tissue samples from the brain, liver, and kidney of each animal also underwent analysis for Pt.

Each tissue sample was washed and stored in deionised water. The tissue was homogenized and digested in re-distilled nitric acid and hydrochloric acid (3:1) for 60 min in a DigiPrep block set (SCP Science) at 95 °C and transferred to a Milestone microwave for 30 min to complete the digestion process. Liquid

samples were micro filtered and analysed using an Agilent 7700X ICP-MS system. There was sufficient brain, liver, and kidney tissue to perform two sets of measurements per tissue sample and to perform an analysis on combined tissue samples across all six animals. Analysis of cochlear tissue was restricted to a single measurement due to the limited size of the cochlear samples. Pt trace analysis was reported as the mass of Pt per half cochlea or the mean mg/kg for brain, liver, and kidney tissue.

### 2.12. Statistical analysis

All statistical analysis was performed using SigmaPlot version 13.0 (Systat Software, Inc.). For all comparisons, the Shapiro–Wilk tested normality and the Brown–Forsythe tested the homogeneity of variance. A  $p \leq 0.05$  indicated significance for all statistical tests. The common ground impedances of control electrodes (from the unstimulated control cochlear array), and unstimulated, flanker, and centre-electrodes (from the chronically stimulated electrode array) were compared between the day that stimulation was turned on (2 weeks after surgery) and the final recorded impedances (prior to termination) using a two-way repeated measures (RM) analysis of variance (ANOVA). Two-way RM ANOVA was also used to compare the CSC, CIL, and EIS at 100 Hz, 1 kHz, 10 kHz, and 100 kHz of electrodes from the stimulated arrays versus unstimulated arrays at 2 weeks, 3 months, and 6 months post-surgery, as well as to compare the EIS equivalent circuit model parameters over time, and the tissue response in unstimulated and stimulated cochleae at various locations of the cochlea. If significant, all pairwise comparisons were performed using the Holm–Sidak method. EIS at 1 Hz were recorded only at 6 months and was compared between electrodes from stimulated and unstimulated arrays using the Welch's t-test. A two-way RM ANOVA was used to compare ECAP thresholds from stimulated and control cochleae recorded at the onset and on completion of the chronic stimulation program. Corrosion scores were correlated with stimulation charge density using least squares regression. Tissue response, corrosion score, and final impedance were correlated using Pearson's Product-Moment correlation. Analysis of AN density were made by comparing each region of the stimulated cochlea with its unstimulated control cochlea using a paired t-test. Finally, trace levels of Pt within cochlea were compared between stimulated and unstimulated controls using Mann–Whitney Rank Sum Test. Data are presented as mean and standard error of the mean (sem). All histological measurement (including AN survival, tissue response, thickness of the macrophage zones and Particulate Pt), and SEM analysis of the Pt electrodes were performed using appropriate blinded techniques.

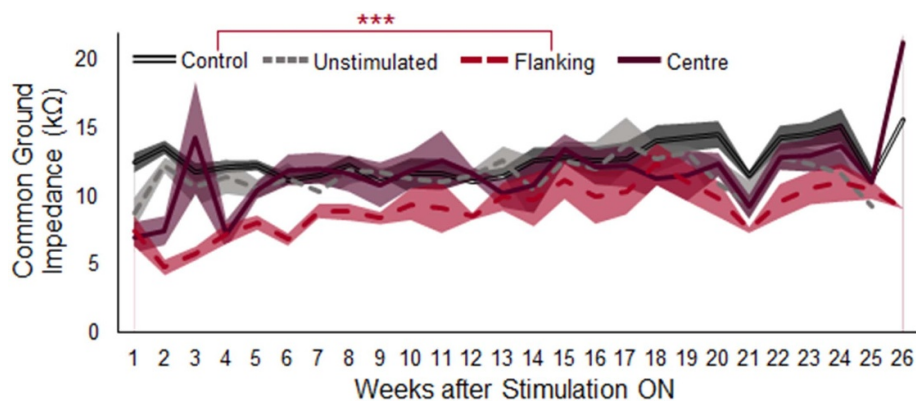


**Figure 3.** Common ground impedances measured throughout the stimulation program. Mean ( $\pm$ sem) impedances of control (from unstimulated array; double line), unstimulated (from stimulated array; short dashed), flanker (long dashed), and centre-electrodes (solid line). The impedances were smoothed by binning the values into 7 d increments and taking the mean of the impedances from each animal, then taking the group mean of the impedance from all animals. The shaded region indicates the sem in each bin.

### 3. Results

#### 3.1. Stimulation program

Five out of the six animals were stimulated for 24–26 weeks. In one animal (HCD\_1), the stimulation program was terminated at 7 weeks due to leadwire damage. During the stimulation program, electrode configurations required updating due to several electrodes exceeding 20 k $\Omega$  or below 1.2 k $\Omega$ . At the 6 months post-surgery time point, 12 out of the 20 centre-electrodes (5 out of 6 cats) were no longer viable for stimulation or electrochemical recordings. In instances where the centre-electrode was unavailable, a bipolar configuration was used for electrochemical recordings.

#### 3.2. Electrode impedance

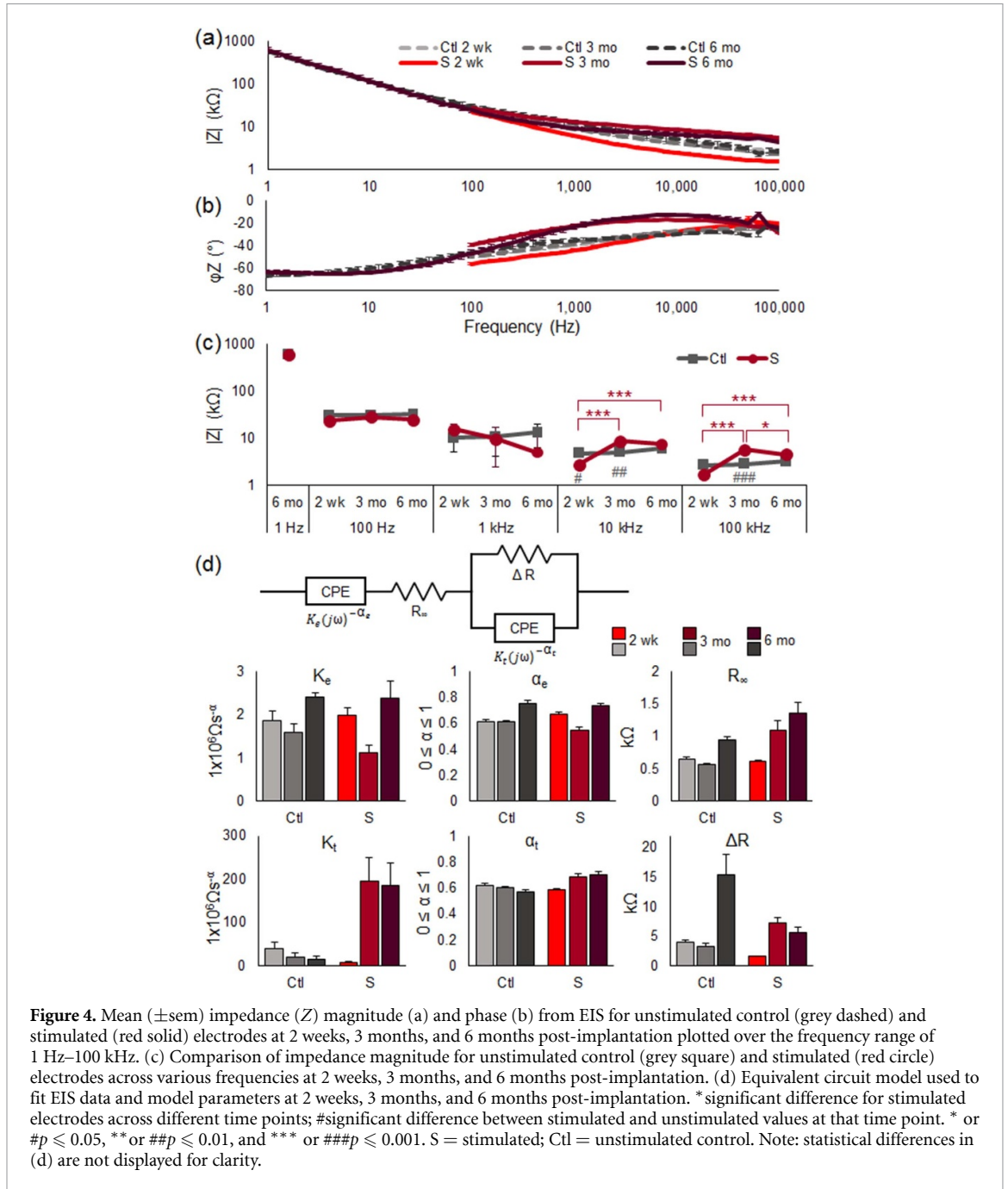
Common ground impedances for all control electrodes from the unstimulated array, and unstimulated, flanker, and centre-electrodes from the stimulated array were recorded immediately prior to the commencement of stimulation (2 weeks after surgery;  $n = 131$ ), and were compared to the final impedances recorded on completion of each animal's stimulation program for cats HCD\_2 to HCD\_6 ( $n = 118$ ; figure 3). There were no significant interaction effects of time versus the stimulation charge density for each electrode ( $p = 0.311$ ), nor was there an effect of time on the electrode impedances ( $p = 0.06$ ). However, control electrodes had a small but significant increase in impedance compared with flanker-electrodes ( $p < 0.001$ ; Ctl =  $12.6 \pm 0.4$  k $\Omega$ ;  $F = 9.5 \pm 0.5$  k $\Omega$ ). A moving average of the impedances for control, unstimulated, flanker, and centre-electrodes over the implant duration is shown in figure 3.

#### 3.3. In vivo electrochemical measurement

Statistical comparisons for all electrochemical measures excluded HCD\_1 because this animal did not

have recordings from the 3 and 6 month time points. At 2 weeks, 3 months, and 6 months post-surgery, there were 18, 17, and 15 electrode configurations recorded from unstimulated control cochleae and 20, 15, and 12 electrode configurations recorded from the stimulated electrodes, respectively.

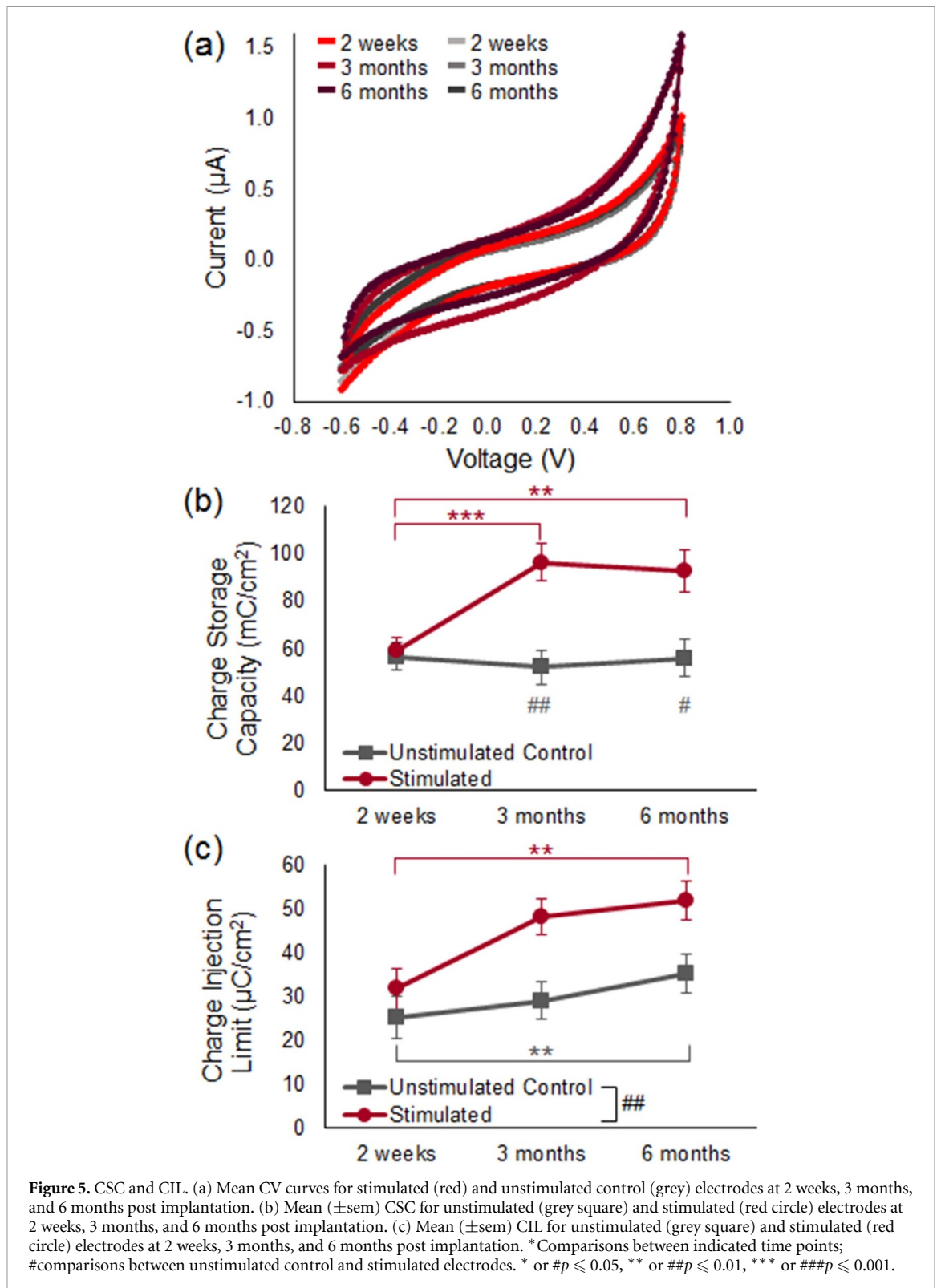
The mean ( $\pm$ sem) magnitude and phase of the impedance from EIS are illustrated in figures 4(a) and (b). Comparisons of the impedance magnitude over time at select frequency values are shown in figure 4(c). The low-frequency spectra (1–100 Hz) were only measured at the 6 month termination. The impedance magnitude at 1 Hz was not different between stimulated ( $EIS_{1\text{Hz}_S} = 605 \pm 12$  k $\Omega$ ) and unstimulated controls ( $EIS_{1\text{Hz}_{\text{Ctl}}} = 600 \pm 38$  k $\Omega$ ) electrodes ( $p = 0.97$ ). At 100 Hz, the impedance magnitude of stimulated electrodes ( $EIS_{100\text{Hz}_S} = 25.1 \pm 2.4$  k $\Omega$ ) was significantly lower than unstimulated control electrodes ( $EIS_{100\text{Hz}_{\text{Ctl}}} = 31.1 \pm 2.2$  k $\Omega$ ) according to two-way RM ANOVA ( $p = 0.049$ ) but not post-hoc tests ( $p = 0.071$ ). The impedance magnitude at 10 kHz increased and was significantly different over time for stimulated electrodes only ( $p < 0.001$  for 2 weeks [ $EIS_{10\text{kHz}_{S2W}} = 2.7 \pm 0.5$  k $\Omega$ ] compared to 3 months [ $EIS_{10\text{kHz}_{S3M}} = 8.7 \pm 0.7$  k $\Omega$ ] and 6 months [ $EIS_{10\text{kHz}_{S6M}} = 7.2 \pm 0.8$  k $\Omega$ ]). Furthermore, the impedance magnitude of stimulated electrodes was significantly different from unstimulated control electrodes at 2 weeks and 3 months ( $p < 0.03$ ;  $EIS_{10\text{kHz}_{\text{Ctl}2W}} = 4.7 \pm 0.5$  k $\Omega$ ;  $EIS_{10\text{kHz}_{\text{Ctl}3M}} = 5.0 \pm 0.7$  k $\Omega$ ). The impedance magnitude of stimulated electrodes at 100 kHz increased with time, where significant differences were found between 2 weeks ( $EIS_{100\text{kHz}_{S2W}} = 1.7 \pm 0.2$  k $\Omega$ ) and 3 ( $EIS_{100\text{kHz}_{S3M}} = 5.6 \pm 0.3$  k $\Omega$ ) and 6 ( $EIS_{10\text{kHz}_{S6M}} = 4.5 \pm 0.4$  k $\Omega$ ) months ( $p < 0.001$ ). There was also a significant difference between 3 and 6 months ( $p = 0.032$ ). Finally, stimulated electrodes were significantly different from unstimulated control electrodes at 3 months only ( $p < 0.001$ ;



EIS<sub>100kHz\_Ctl3M</sub> =  $2.8 \pm 0.3$  k $\Omega$ ). All other comparisons were not significant ( $p > 0.05$ ).

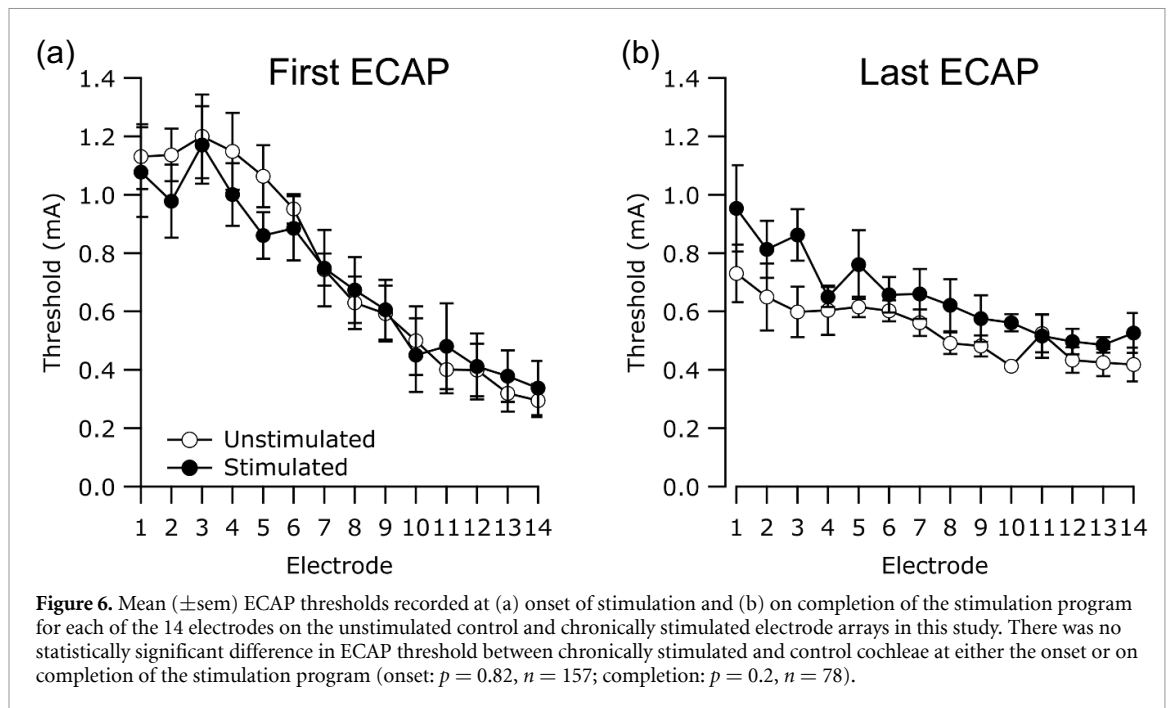
Equivalent circuit modelling of the EIS data was performed to help provide a physical basis for the impedance behavior at each time point (figure 4(d)). The model chosen was the one determined by Lempka *et al* as the best fit from a range of models investigated in their work [25].  $K_e$  and  $\alpha_e$  are components of the CPE for the electrode–electrolyte interface, and  $K_t$  and  $\alpha_t$  are components of the CPE for the tissue layer according to equation (1) [26, 27].  $R_\infty$  and  $\Delta R$  are the resistive components of the tissue layer at different frequencies.  $K_e$  displayed a time effect only, where the value at 2 weeks ( $K_{e2wk} = 2.0 \pm 0.2 \times 10^6 \Omega s^{-\alpha}$ )

was significantly different and higher than at 3 months ( $K_{e3mo} = 1.2 \pm 0.2 \times 10^6 \Omega s^{-\alpha}$ ;  $p = 0.016$ ) and the value at 3 months was significantly different and lower than at 6 months ( $K_{e6mo} = 2.3 \pm 0.2 \times 10^6 \Omega s^{-\alpha}$ ;  $p = 0.007$ ).  $\alpha_e$  also only displayed a time effect where the value at 2 weeks ( $\alpha_{e2wk} = 0.64 \pm 0.02$ ) was significantly different from 3 ( $\alpha_{e3mo} = 0.57 \pm 0.02$ ;  $p = 0.009$ ) and 6 months ( $\alpha_{e6mo} = 0.73 \pm 0.02$ ;  $p = 0.011$ ), and the value at 3 months was also different from 6 months ( $p < 0.001$ ).  $R_\infty$  did not have any interaction effects. Overall, the unstimulated control electrodes ( $R_{\infty Ctl} = 0.70 \pm 0.08$  k $\Omega$ ) had a significantly lower  $R_\infty$  than stimulated electrodes ( $R_{\infty S} = 1.01 \pm 0.08$  k $\Omega$ ;  $p = 0.011$ ). Additionally,



$R_{\infty}$  at 2 weeks ( $R_{\infty 2\text{wk}} = 0.63 \pm 0.09 \text{ k}\Omega$ ) at 3 months ( $R_{\infty 3\text{mo}} = 0.78 \pm 0.11 \text{ k}\Omega$ ) were significantly lower than at 6 months ( $R_{\infty 6\text{mo}} = 1.16 \pm 0.12 \text{ k}\Omega$ ;  $p = 0.003, 0.049$ , respectively). For stimulated electrodes,  $K_t$  was significantly higher at 3 months ( $K_{t3\text{mo}} = 189.4 \pm 50.1 \times 10^6 \Omega \text{s}^{-\alpha}$ ) and 6 months ( $K_{t6\text{mo}} = 186.5 \pm 57.0 \times 10^6 \Omega \text{s}^{-\alpha}$ ) compared to 2 weeks ( $K_{t2\text{wk}} = 9.0 \pm 1.9 \times 10^6 \Omega \text{s}^{-\alpha}$ ;  $p = 0.009, 0.014$ , respectively). Furthermore,

stimulated electrodes had a significantly higher  $K_t$  than unstimulated controls at 3 ( $p = 0.026$ ) and 6 months ( $p = 0.061$ ). At 6 months post-implantation ( $\alpha_{t6\text{mo}} = 0.72 \pm 0.04$ ),  $\alpha_t$  was significantly higher than at 2 weeks ( $\alpha_{t2\text{wk}} = 0.57 \pm 0.03$ ;  $p = 0.005$ ) and 3 months ( $\alpha_{t3\text{mo}} = 0.70 \pm 0.03$ ;  $p = 0.003$ ) for stimulated electrodes. Additionally, there was a significant difference between unstimulated control and stimulated electrodes at 3 ( $p = 0.036$ ) and



6 months ( $p = 0.009$ ). Finally,  $\Delta R$  for unstimulated control electrodes had a large increase at 6 months ( $\Delta R_{U6mo} = 15.2 \pm 1.9 \text{ k}\Omega$ ) that was significantly higher than at 2 weeks ( $\Delta R_{U2wk} = 4.2 \pm 1.4 \text{ k}\Omega$ ;  $p < 0.001$ ) and 3 months ( $\Delta R_{U3mo} = 4.7 \pm 1.8 \text{ k}\Omega$ ;  $p < 0.001$ ), as well as significantly higher than  $\Delta R$  for stimulated electrodes at 6 months ( $p = 0.015$ ). For stimulated electrodes,  $\Delta R$  increased significantly at 3 ( $\Delta R_{S3mo} = 7.7 \pm 2.0 \text{ k}\Omega$ ) and 6 months ( $\Delta R_{S6mo} = 7.9 \pm 2.3 \text{ k}\Omega$ ) compared to 2 weeks post-implantation ( $\Delta R_{U3mo} = 1.5 \pm 1.5 \text{ k}\Omega$ ;  $p = 0.05$ ,  $0.045$ , respectively).

The mean CV curve for unstimulated control electrodes and stimulated electrodes at 2 weeks, 3 months, and 6 months is shown in figure 5(a). The CSC of unstimulated control electrodes ( $CSC_{Cil} = 54.7 \pm 7.7 \text{ mC cm}^{-2}$ ) did not significantly change over time ( $p > 0.95$ ) and were similar to the CSC of stimulated electrodes at 2 weeks—prior to the stimulation program commencing ( $CSC_{S2W} = 58.6 \pm 5.4 \text{ mC cm}^{-2}$ ;  $p = 0.841$ ; figure 5(b)). The CSC of stimulated electrodes increased significantly between 2 weeks and 3 months ( $p < 0.001$ ;  $CSC_{S3M} = 96.2 \pm 7.9 \text{ mC cm}^{-2}$ ) and remained high at 6 months ( $CSC_{S6M} = 92.7 \pm 8.9 \text{ mC cm}^{-2}$ ;  $p = 0.774$  for comparison between 3 and 6 months;  $p = 0.004$  for comparison between 2 weeks and 6 months). Additionally, the CSC of stimulated electrodes significantly differed from unstimulated control electrodes at 3 months ( $CSC_{Cil3M} = 52.0 \pm 7.2 \text{ mC cm}^{-2}$ ;  $p = 0.005$ ) and 6 months ( $CSC_{Cil6M} = 55.8 \pm 7.7 \text{ mC cm}^{-2}$ ;  $p = 0.031$ ).

For both stimulated and unstimulated control electrodes, the CIL increased significantly between 2 weeks and 6 months ( $CIL_{S2W} = 31.7 \pm 4.7 \mu\text{C cm}^{-2}$ ;

$CIL_{S6M} = 51.8 \pm 4.5 \mu\text{C cm}^{-2}$ ;  $CIL_{Cil2W} = 25.2 \pm 4.8 \mu\text{C cm}^{-2}$ ;  $CIL_{Cil6M} = 35.1 \pm 4.4 \mu\text{C cm}^{-2}$ ;  $p = 0.005$ ; figure 5(c)). Stimulated electrodes had a larger CIL that was significantly different from the CIL of unstimulated control electrodes ( $CIL_S = 43.9 \pm 3.4 \mu\text{C cm}^{-2}$ ;  $CIL_{Cil} = 29.8 \pm 3.4 \mu\text{C cm}^{-2}$ ;  $p = 0.006$ ). There were no interaction effects of stimulation states (stimulated or unstimulated control) with time ( $p = 0.341$ ); therefore, further pairwise comparisons were not made.

### 3.4. Electrically-evoked responses

There was no statistically significant difference in ECAP threshold between chronically stimulated and control cochleae at either the onset or on completion of the stimulation program (figure 6). Furthermore, there was no significant interaction between electrode and side ( $p > 0.1$ ), indicating the chronically stimulated electrodes did not exhibit an increase in threshold. Finally, there was a significant effect of electrode at first recording ( $p < 0.001$ ), that just failed significance at the last recording ( $p = 0.053$ ); reflecting the lower thresholds associated with more apically located electrodes due to the tapered nature of the scala tympani [19].

### 3.5. Cochlear pathology

#### 3.5.1. General cochlear pathology

There was evidence of minor electrode insertion trauma in the UB turn of three of the stimulated cochleae in the present study (HCD\_3, left; HCD\_5, left; HCD\_6, right); therefore, while the great majority of the tissue response reported here was associated with the chronically implanted electrode array and/or the

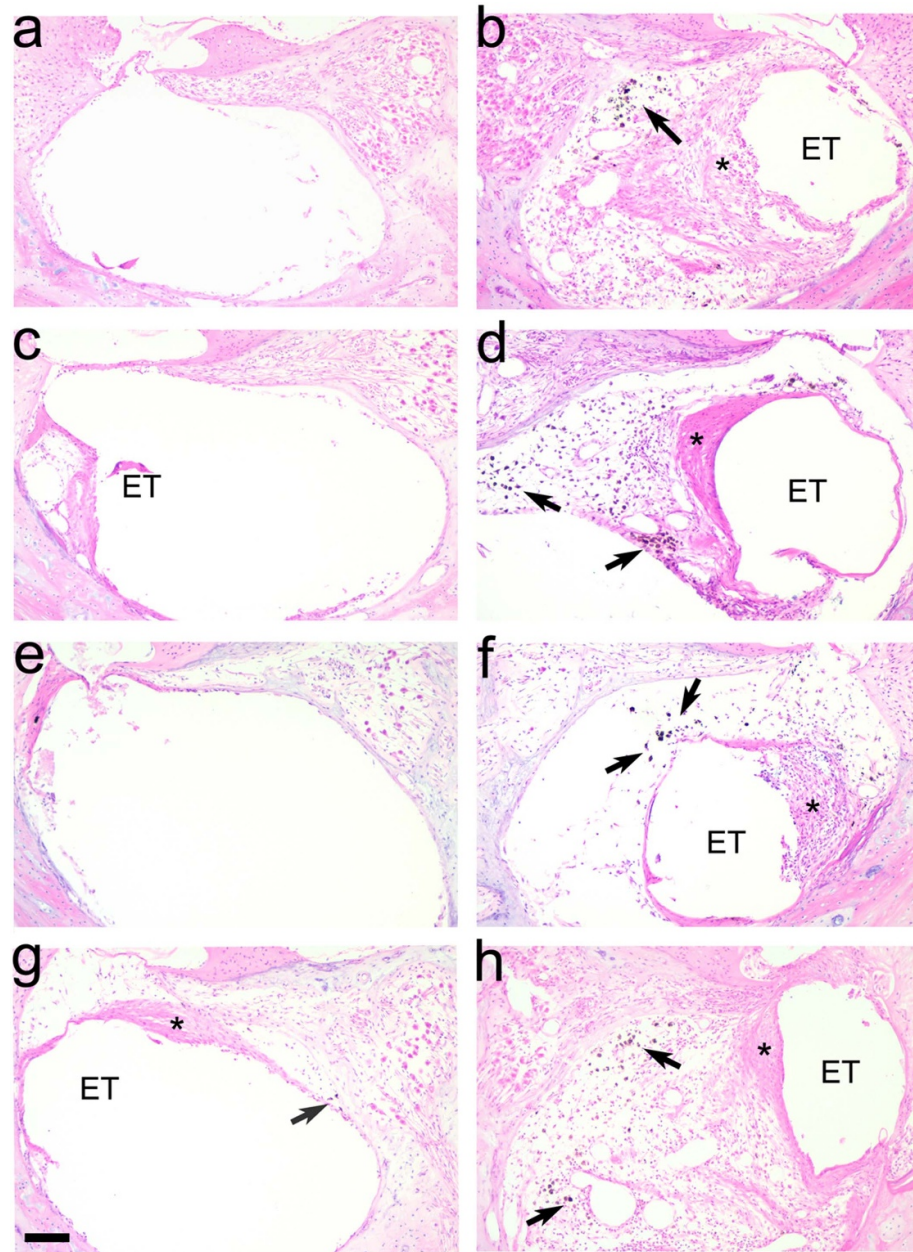


**Figure 7.** Representative micrographs illustrating the typical tissue response within the UB turn scala tympani of implanted unstimulated control (left), and chronically stimulated cochleae (right). The control cochleae exhibited a relatively minimal tissue response with some cochleae showing small amounts of particulate material within the scala tympani (arrow). In contrast, all stimulated cochleae exhibited an extensive tissue response, including a zone of macrophages (\*) and clear evidence of particulate material in the tissue response (arrows). (a) HCD\_1 control; (b) HCD\_1 stimulated; (c) HCD\_2 control; (d) HCD\_2 stimulated; (e) HCD\_4 control; (f) HCD\_4 stimulated; (g) HCD\_6 control; (h) HCD\_6 stimulated. ET = electrode tract. Arrows show examples of particulate material within the tissue capsule. Scale bar = 100  $\mu\text{m}$ .

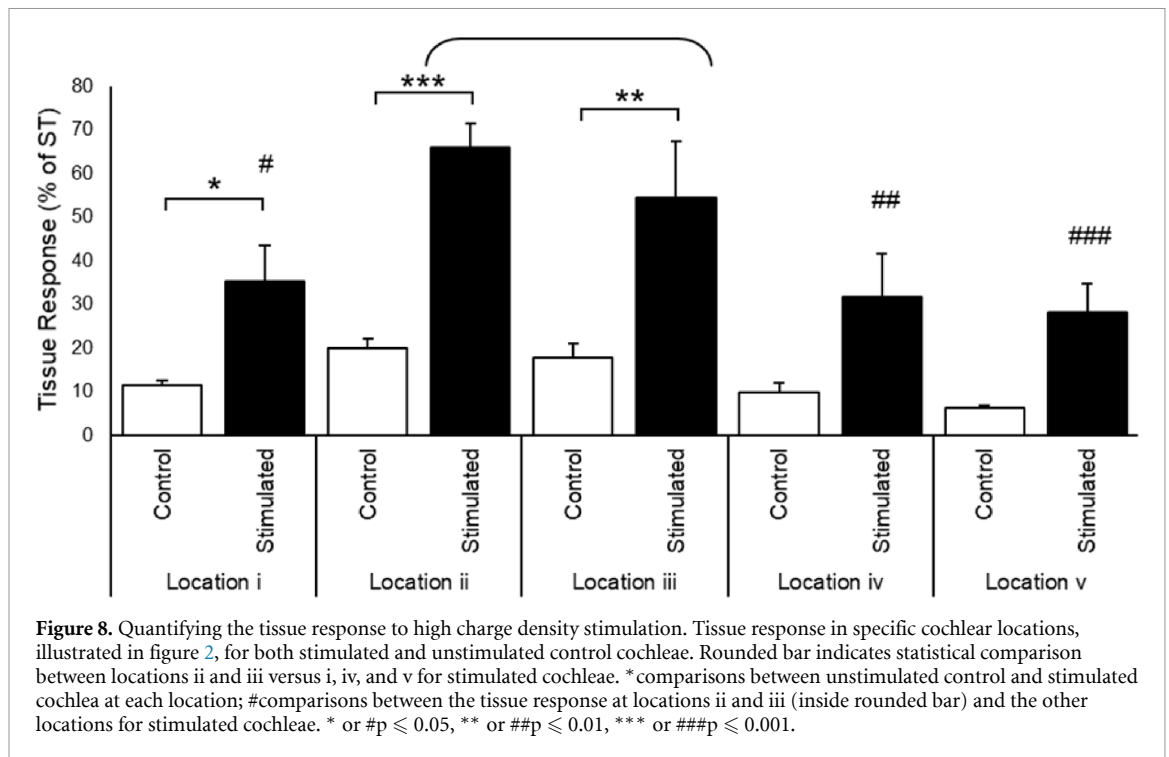
effects of electrical stimulation, in these cochleae localized trauma also contributed to the response.

### 3.5.2. Tissue response

Figure 7 illustrates the typical tissue response observed in the UB turn adjacent to the electrode array in both chronically implanted unstimulated control, and chronically stimulated cochleae. Control cochleae exhibited a relatively minimal tissue response that usually included a fine tissue capsule surrounding the electrode array together with some loose areolar tissue (e.g. figure 7(g)). A more

extensive tissue response was always evident in chronically stimulated cochleae. This typically took the form of a thick, mature tissue capsule surrounding the electrode array forming an electrode tract (ET; e.g. figure 7(b)), with loose vascularized fibrous tissue occupying much of the remainder of the scala tympani.

We quantified the tissue response in each chronically implanted cochlea by measuring the area of the tissue occupying the scala tympani in each of the five cochlear locations illustrated in figure 2 ( $n = 12$  for locations i, ii, and v;  $n = 6$  for locations iii and iv; for



both unstimulated control and stimulated cochleae). The data demonstrated a significant difference in the level of tissue response associated with the chronically stimulated cochlea compared to the implanted unstimulated control ( $p < 0.05$ ; figure 8). Although there is variation due to orientation of the section plane, electrode insertion distance, and cochlear anatomy, cochlear locations can be generally related to electrode position; location i is at the base of the cochlea near the unstimulated electrodes E1 and E2; location ii is near electrodes 9–10 and would be receiving stimulation; location iii is also near stimulating electrodes (~E11, E12); location iv is close to the most apical electrode (E14) and subject to reduced levels of stimulation; finally, location v is typically apical to the electrode array.

Implanted, unstimulated control cochleae did not exhibit a significantly different tissue response across the cochlear regions examined ( $p > 0.2$ ; figure 8). In stimulated cochleae, the most extensive tissue response was in location ii ( $66 \pm 5.5\%$  of area of the scala tympani; figure 8), and was significantly higher than locations i ( $p < 0.001$ ), iv ( $p < 0.001$ ), and v ( $p < 0.001$ ). The second largest tissue response was associated with location iii ( $54 \pm 12.9\%$  of area of the scala tympani; figure 8); this location also exhibited significantly greater tissue response than locations i ( $p = 0.012$ ), iv ( $p = 0.003$ ), and v ( $p < 0.001$ ). Locations ii and iii are proximal to both flanker and centre-electrodes, and would be the two sites subject to the most extensive stimulation in this analysis. The tissue response in locations i ( $p = 0.044$ ), ii ( $p = 0.001$ ), and iii ( $p = 0.006$ ) were significantly larger in the stimulated compared to the unstimulated control cochleae; although, locations iv and v also

showed a trend towards an increased tissue response in the stimulated cochlea compared to the unstimulated cochlea.

There was no evidence of necrosis associated with the Pt–tissue interface in either stimulated or control cochleae. However, there was often a region of macrophages located between the electrode array and the mature fibrous tissue response (e.g. figure 7(h)). The mean thickness of this zone was significantly greater in stimulated ( $86.7 \pm 31.9 \mu\text{m}$ ) than implanted control cochleae ( $22.4 \pm 36.2 \mu\text{m}$ ;  $p = 0.03$ ,  $n = 6$ ).

### 3.5.3. AN survival

Figure 9 illustrates the typical AN survival in the UB turn (i.e. in zones ii–iii adjacent to stimulating electrodes E9–E11) in the present study. The relatively low packing density of ANs, particularly animals HCD\_2–HCD\_6 (figures 9(c)–(l)), reflects the long duration between deafening and termination associated with the present study (>6 months). In contrast, animal HCD\_1 (figures 9(a) and (b)) was deafened for a considerably shorter period (~12 weeks) and displayed greater AN survival in both cochleae. There is close symmetry in AN survival between the stimulated (figures 9(b), (d), (e), (h), (i) and (l)) and the implanted, unstimulated control cochleae (figures 9(a), (c), (f), (g), (j) and (k)).

Quantitative analysis of AN density showed close bilateral symmetry of AN survival in all cochlear sectors except for the apical region (figure 10; LB,  $n = 24$  & 29; UB,  $n = 29$  & 30; LM,  $n = 29$  & 30; UM,  $n = 25$  & 27; A,  $n = 21$  & 22, for implanted, unstimulated control and chronically stimulated cochlea respectively). Importantly, there was no statistically significant difference in AN density between

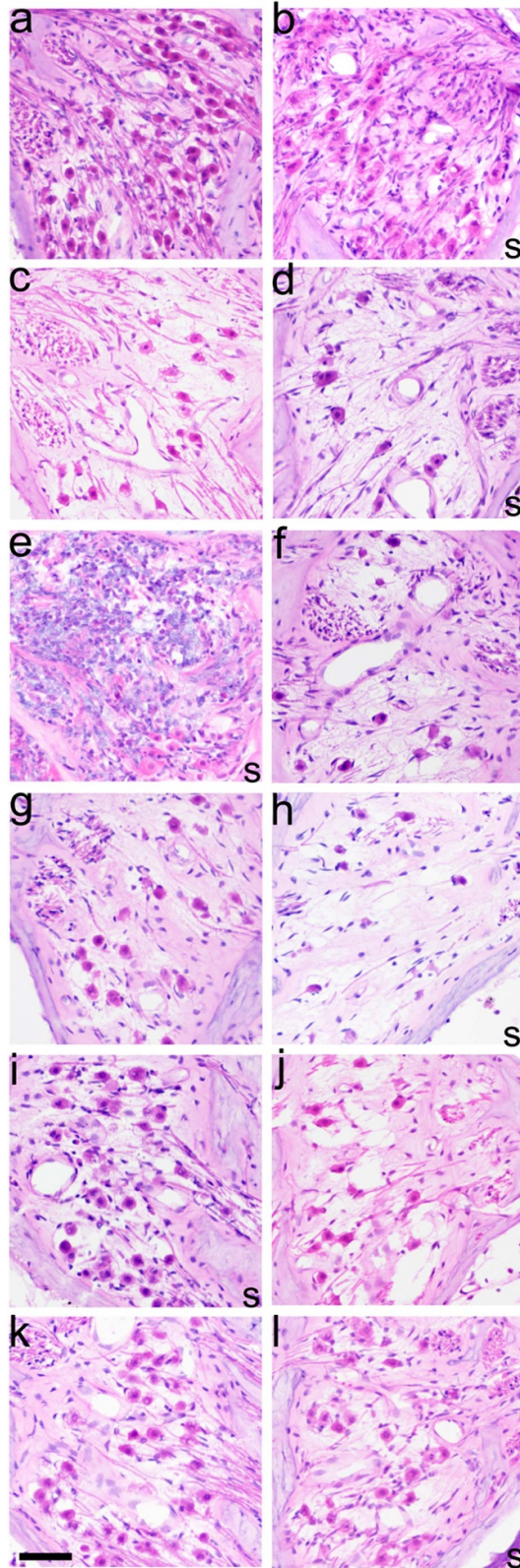


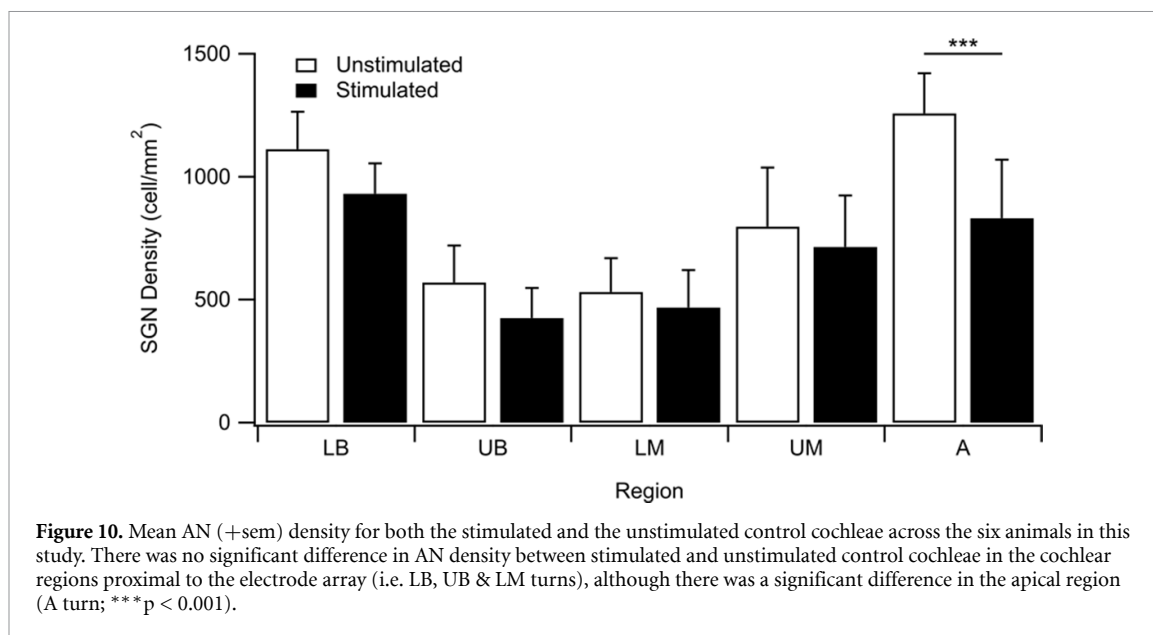
**Figure 9.** Representative micrographs of Rosenthal's canal from the UB turn illustrating the extent of AN survival in the left ((a), (c), (e), (g), (i), (k)) and right ((b), (d), (f), (h), (j), (k), (l)) cochlea in the six animals in this study. HCD\_1 (a), (b); HCD\_2 (c), (d); HCD\_3 (e), (f); HCD\_4 (g), (h); HCD\_5 (i), (j); HCD\_6 (k), (l). The stimulated cochlea in each animal is illustrated (s). Note the inflammatory response in cochlea HCD\_3 left (5e) was associated with electrode insertion trauma at that location. Scale bar = 100  $\mu\text{m}$ .

stimulated and control cochleae in the region of the cochlea subject to electrical stimulation (i.e. LB, UB & LM; figure 10). There was a significant difference in AN density between stimulated and implanted control cochleae in the apical region (A turn;  $p < 0.001$ ; figure 10).

### 3.6. Electrode corrosion

Representative SEM micrographs from four chronically implanted unstimulated control and four chronically stimulated electrodes illustrate the range of Pt corrosion observed in the present study (figure 11). Electrodes from implanted unstimulated control arrays exhibited surface features associated with their manufacture, including lines generated by the laser during removal of the overlying PDMS (e.g. figure 11(a)). Control electrodes from unstimulated control arrays showed no evidence of corrosion (grade 0; e.g. figures 11(a), (c), (e) and (g)); although, some contained an assumed organic material on their surface (grade 1; not illustrated). Unstimulated electrodes on chronically stimulated electrode arrays (e.g. E1 and E2) also showed no evidence of Pt corrosion; however, a greater proportion of these electrodes contained an organic coating (grade 1). The majority of stimulated electrodes showed evidence of Pt corrosion; the extent of the corrosion was dependent on the electrode's stimulation history. The majority of tripole centre-electrodes exhibited widespread corrosion (grade 4; e.g. figures 11(d), (f) and (h)); however, more localised corrosion was sometimes observed (grade 3; e.g. figure 11(b)). Flanker-electrodes, stimulated at approximately half the charge density of centre-electrodes, showed less Pt corrosion than centre-electrodes (typically grades 1–2; not illustrated). Finally, in a small number of cases the Pt surface was covered with corrosion products and/or tissue that required removal prior to examination of the Pt surface (e.g. figure 11(d)). In these examples the underlying Pt surface was typically corroded.

The SEM surface grading of the electrodes was compared with their stimulation histories (figure 12). There was a significant difference in the level of surface corrosion across electrode groups ( $p < 0.001$ ;  $n = 84$  control electrodes;  $n = 12$  unstimulated electrodes;  $n = 46$  flanker electrodes;  $n = 21$  centre electrodes). There was a statistically significant difference in corrosion grading between tripole centre-electrodes (corrosion grade 3–4) versus electrodes from unstimulated control arrays (grade 0–1;  $p < 0.001$ ), non-stimulated electrodes on chronically stimulated arrays (grade 0–1;  $p < 0.001$ ), and flanker-electrodes on chronically stimulated arrays (grade 1–2;  $p < 0.001$ ). Flanker-electrodes showed a significant difference to control electrodes ( $p < 0.001$ ); although were not significantly different to unstimulated electrodes ( $p = 0.24$ ).



Corrosion scores correlated with stimulation charge density; more corrosion was observed on electrodes with a higher charge density ( $R^2 = 0.91$ ). Finally, there was no significant effect of implant duration ( $p = 0.54$ ), implying that corrosion of the Pt surface occurs rapidly following onset of the stimulation.

Figure 13 illustrates the relationship between tissue response, final impedance and the extent of electrode corrosion for the four electrode categories (unstimulated control, unstimulated, flanker, and centre) in the present study for each cat. The tissue response moderately correlated with the electrode corrosion score ( $r = 0.61$ ;  $p = 0.0015$ ); however, the final impedance recording had a weak correlation with corrosion scores ( $r = 0.29$ ;  $p = 0.19$ ) and poor correlation with the tissue response ( $r = 0.06$ ;  $p = 0.78$ ).

### 3.7. Analysis of particulate deposits

Representative photomicrographs illustrating particulate matter in both control and stimulated cochleae are illustrated in figure 14. Histological examination of these particulate deposits revealed they occurred in two forms: the majority of the material appeared to be of sub-micron dimensions and readily phagocytosed by macrophages (e.g. figures 14(ai) and (bi)), while there were occasional larger deposits ( $\sim 20 \mu\text{m}$  in length) that had not undergone phagocytosis (e.g. figure 14(bi)). The particulate material we have described in previous studies were localized close to the electrode tract [16]; however, in the present study the deposits associated with the chronically stimulated cochleae were located more distal to the electrode tract within the scala tympani (e.g. figure 14(b)). There was no evidence of particulate material proximal to ANs within Rosenthal's canal. Examination of this material using SEM-EDS in both

chronically implanted unstimulated and chronically stimulated cochleae identified the particulate as Pt (data not illustrated).

There was clear evidence of Pt deposits in all chronically stimulated cochleae. Pt deposits were also evident in chronically implanted unstimulated control cochleae, although significantly less than observed in stimulated cochleae ( $p = 0.001$ ;  $n = 6$ , figure 15).

### 3.8. Trace analysis of Pt

Trace levels of Pt were identified in all cochleae (table 2). Stimulated cochleae contained significantly greater levels of Pt than implanted unstimulated control cochleae ( $p < 0.002$ ). ICP-MS was also used to determine whether Pt was present in the brain, liver and kidney of all animals in this study. While two of the six animals showed trace levels of Pt in the kidney, there was no detectible Pt in the brain or liver of any animal (table 2).

## 4. Discussion

The present study examined the effects of long-term intracochlear stimulation using Pt electrodes at a charge density well above currently accepted safe guidelines for cochlear implants [7, 11]. Cochleae stimulated continuously for periods of up to 6 months showed extensive Pt corrosion product within the scala tympani. Notably, small amounts of particulate Pt were also observed in the tissue capsule of chronically implanted unstimulated control cochleae. ICP-MS analysis confirmed the presence of Pt in all cochleae, although stimulated cochleae had significantly greater levels than the implanted unstimulated controls. Examination of the electrode surface showed significant levels of corrosion for electrodes stimulated at a charge density

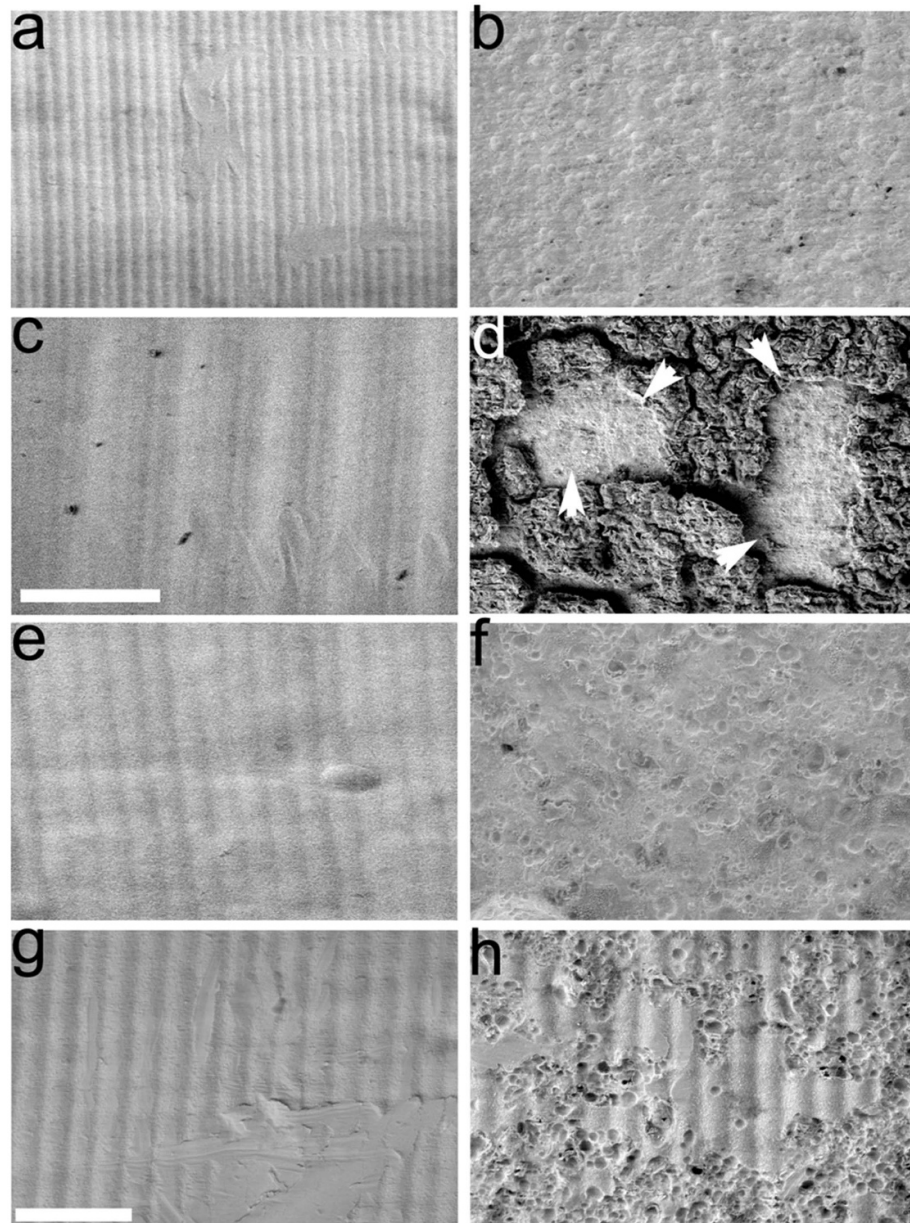


**Figure 11.** SEM images illustrating the electrode surface of four implanted, unstimulated electrodes from control electrode arrays ((a), (c), (e), and (g)), and four chronically stimulated centre-electrodes ((b), (d), (f), (h)). (a) HCD\_2\_left E10 (corrosion grade: 0); (b) HCD\_2\_right E6 (grade: 3); (c) HCD\_6\_left E10 (grade: 0); (d) HCD\_6\_right E10 (grade: 4). This electrode exhibited a coating with evidence of corrosion on the underlying Pt surface (arrows). We did not evaluate the nature of the coating; (e) HCD\_1\_left E10 (grade: 0); (f) HCD\_1\_right E10 (grade: 4); (g) HCD\_3\_right E4 (grade: 0); (h) HCD\_3\_left E4 (grade: 4). Scale bar: a – d = 50  $\mu\text{m}$ ; e – h = 20  $\mu\text{m}$ .

of 267  $\mu\text{C cm}^{-2} \text{ phase}^{-1}$ , while unstimulated electrodes showed no surface corrosion. Consistent with corrosion resulting in an increased effective surface area, the stimulated electrodes also presented with an increased CSC and CIL. There was a significantly greater tissue response in stimulated versus implanted unstimulated cochleae, which was also indicated by the EIS equivalent circuit modelling. However, there was no evidence of the focal necrosis we reported previously following shorter duration stimulation [16, 17]. Despite 26 weeks of continuous stimulation at these high charge densities evoking a significant tissue response and extensive Pt corrosion product, there was no evidence of a reduction in AN density

or loss of neural function. Finally, there was no evidence of Pt in brain or liver tissue in the chronically stimulated animals; however, trace levels of Pt were observed in the kidney of two animals.

#### 4.1. Pt dissolution *in vivo*

We evaluated the extent of Pt corrosion using three measures: (a) the amount of Pt corrosion product observed histologically; (b) the extent of Pt corrosion associated with the surface of the electrodes examined under SEM; and (c) trace analysis of Pt in cochleae measured using ICP-MS. All three techniques showed a significant increase in the level of Pt corrosion associated with electrical stimulation.

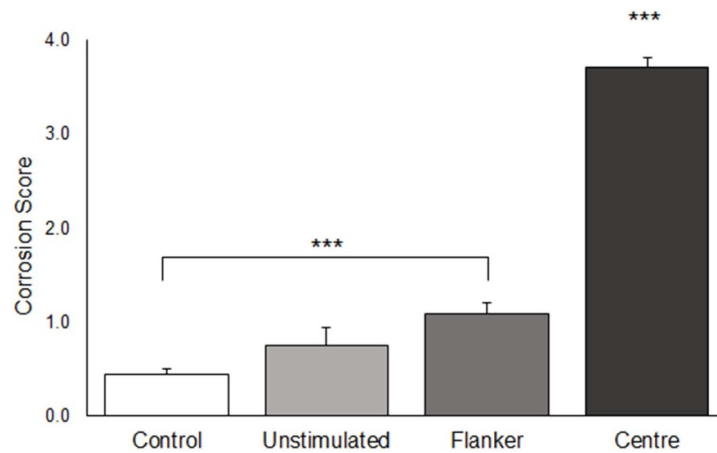


**Figure 12.** Corrosion grade showing mean ( $\pm$  sem) corrosion scores for each electrode cohort in this study. Control = electrodes from implanted unstimulated control array; Unstimulated = electrodes from chronically stimulated array. \*\*\* $p \leq 0.001$ . Symbols above centre bar indicate comparisons between centre-electrodes and all other groups.

As we noted previously [16], although centre-electrodes of a tripole were stimulated using cathodic first pulses they demonstrated the most significant levels of corrosion. Pt corrosion has been conventionally associated with anodic reactions [3, 33], however, more recently Pt corrosion mechanisms have also been described under cathodic pulsing conditions [34, 35]. Our results support the notion that Pt ions can be released into solution under both anodic and cathodic pulsing conditions. Whether one or both mechanisms play a role appears to depend on the specific conditions at a particular electrode.

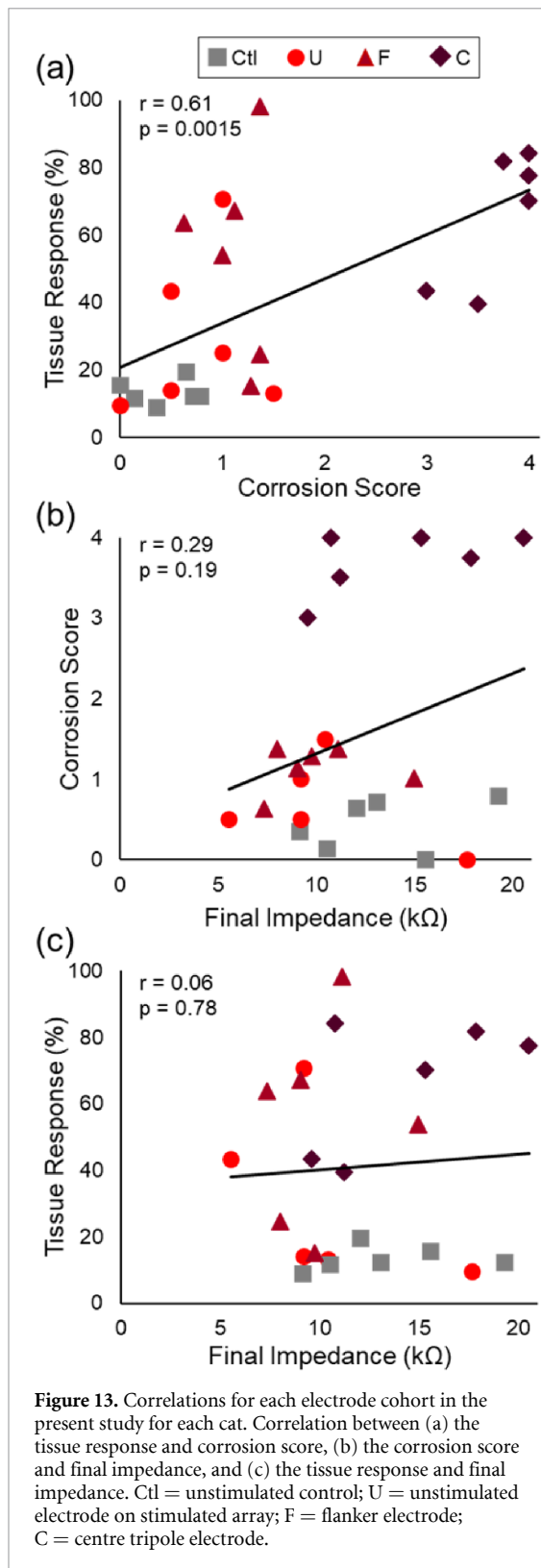
The formation of particulate Pt within the cochlea may be associated with the reduction of Pt ions back onto the bulk Pt electrode during the cathodic phase of the pulse [36], and the electroplated Pt then flaking off into the adjacent tissue [16]. The amount of redeposited Pt would be dependent on the amount of Pt ions proximal to the electrode when its potential becomes sufficiently negative to reduce Pt ions to Pt. Alternatively, it is possible that Pt ions crystallise into a metallic form. The hydroxide complexes of Pt, in particular, are more soluble in high pH conditions [37] and these conditions exist at cathodic first centre-electrodes [5, 38].  $\text{Pt}(\text{OH})_x$  ions that are soluble near the centre-electrode will be less soluble as they diffuse to the more neutral pH conditions that exist distal to the electrode surface where they may precipitate out as solid Pt.

The particulate Pt observed in the present study were similar in appearance to the deposits we have described previously [16, 17]; the majority of Pt had been phagocytosed, although a small number of larger particles were present within the tissue capsule. One difference in the results between the present study and our previous reports is the distribution of the particulate Pt within the scala tympani. Our previous shorter-term studies reported Pt located at the electrode–tissue interface. In contrast, the present

results consistently showed the accumulation of particulate Pt distal to the electrode–tissue interface, yet still contained within the foreign body response in the scala tympani. The present result is consistent with clinical reports of particulate Pt distribution in long-term cochlear implant users [14].

The apparent migration of particulate Pt from the electrode–tissue interface to a more distal site within the scala tympani implies that the majority of Pt dissolution occurred early during the stimulation program. This observation is consistent with previous *in vivo* studies that showed a rapid increase in Pt corrosion product following onset of stimulation [39], with the rate of dissolution decreasing during the course of stimulation [40]. Further support for this observation comes from the trace levels of Pt measured in stimulated cochleae in the present study (table 2); while there was considerable individual variability, HCD\_1, which was stimulated for 7 weeks, had trace levels of Pt greater than the mean for the remaining five animals that were stimulated for  $\sim 26$  weeks. However, it is important to note that the levels of Pt per mg per half cochlea observed in the present study were more than an order of magnitude greater than the levels we reported in guinea pigs following 4 weeks of stimulation [16, 17]. Although there were twice as many tripoles per half cochlea used for stimulation in the present study, this alone does not account for the difference, implying that longer stimulation durations result in more dissolved Pt.

The charge density used to stimulate Pt electrodes had a significant effect on the extent of surface corrosion examined under SEM; centre-electrodes stimulated at  $267 \mu\text{C cm}^{-2} \text{ phase}^{-1}$  exhibited extensive surface corrosion, while flanker-electrodes stimulated at  $\sim 133 \mu\text{C cm}^{-2} \text{ phase}^{-1}$ , and unstimulated electrodes showed little or no corrosion. As noted above, Pt was previously thought to dissolve more readily under anodic/acidic conditions, so it was



somewhat unexpected that the cathodically pulsed centre-electrodes showed such a high rate of dissolution. However, the present results are consistent with our previous findings following 28 d of stimulation using a wider range of charge densities [16, 17], and supports a high pH, cathodic Pt dissolution process [34, 35].

While there are a number of reports describing Pt corrosion product within tissue following periods of electrical stimulation [16, 17, 39, 40], it is noteworthy that the present study also showed evidence of Pt within implanted, unstimulated control cochleae. Two previous studies have also described Pt dissolution of unstimulated or lightly stimulated Pt electrodes [41, 42]; notably, in both cases the electrodes were implanted for years.

This finding suggests that in the absence of electrical stimulation, Pt electrodes may undergo some corrosion during long-term passive implantation. However, there are a number of potential sources that may have contributed to the dissolution of Pt observed in the present study. First, it is possible that small fragments of the metal resided on the electrode surface following manufacture and these flaked off after implantation into the cochlea [13]. This is unlikely as the electrodes were subject to an extensive cleaning program, including sonication, prior to implantation. Furthermore, the nature of the particulate Pt observed histologically were sub-micron in size and phagocytosed; Pt fragments produced during manufacture are likely to be considerably larger. Second, although the implanted, unstimulated electrode arrays were not subject to chronic periods of stimulation, they were acutely stimulated at three time points during the study in order to perform EIS, CV, and VT measurements. This potential source of Pt corrosion is also unlikely as there was no evidence of Pt corrosion in a chronic study comprising multiple electrochemical recordings similar to those performed in the present study [23].

Finally, the electrode contacts in this study were made from 99.95% pure Pt, which is the material used in the contemporary products of all major cochlear implant manufacturers [43–45]. Other contact materials, typically 10%–30% iridium (Ir) alloyed with Pt, are used in other neural stimulator applications such as pacemakers, often for their improved mechanical characteristics. Based on *in vitro* evidence [46, 47], it may be that Ir alloys of Pt offer improved dissolution performance over pure Pt. However, we are not aware of any *in vivo* evidence to date where this has been confirmed.

#### 4.2. Phagocytosis of Pt

The majority of Pt observed within cochleae had undergone phagocytosis by macrophages within the scala tympani, whereby particles are engulfed into phagosomes within the cytoplasm [48]. Macrophages detect cellular debris and pathogens via chemoattractants; however, they also actively probe their microenvironment for inert targets [49]. Presumably, particulate Pt was engulfed via this active probing mechanism. Once engulfed, organic material is gradually digested within the phagosome; however, it is assumed that inert material such as Pt are not digested. While the long-term status of phagosomal

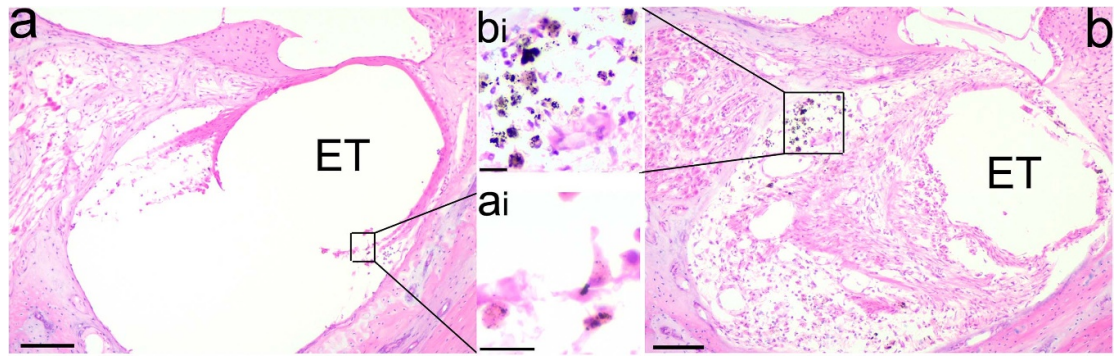


**Figure 14.** Representative micrographs illustrating the extent and nature of particulate deposits in implanted unstimulated control and chronically stimulated cochleae. (a) UB turn of control cochlea HCD\_5 illustrating the presence of an electrode tract (ET) containing a small region of phagocytosed particulate material illustrated at higher magnification in the inset (ai). This cochlea had been implanted for 24 weeks. (b) UB turn of chronically stimulated cochlea HCD\_1. Despite only 7 weeks of stimulation there was extensive particulate material present in the scala tympani. Note that the majority of this material is located distal to the electrode tract. The extent and distribution of the particulate material observed in this example was similar to that observed in all other chronically stimulated cochleae. The majority of the particulate material had been phagocytosed by macrophages within the scala tympani (inset (bi)). Scale bars: (a) and (b) = 100  $\mu\text{m}$ ; (ai) and (bi) 20  $\mu\text{m}$ .

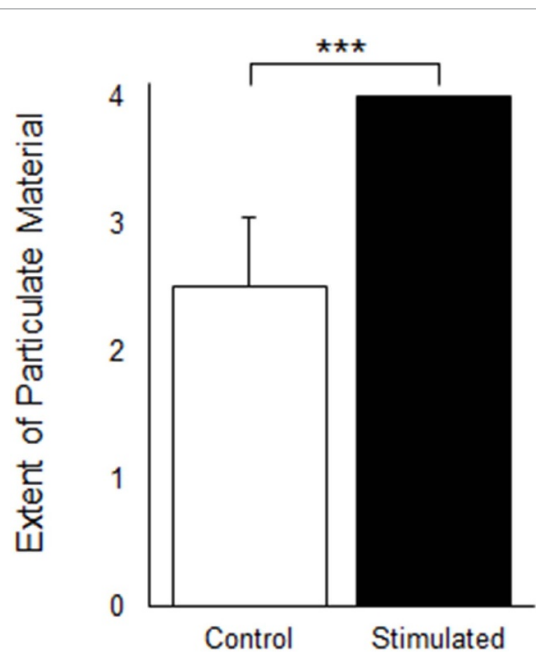


**Figure 15.** Mean (+sem) score of the qualitative estimate of particulate Pt present in implanted unstimulated control cochleae and chronically stimulated cochleae. Note that all stimulated cochleae were graded 4 (widespread particulate material present) and therefore the sem for this cohort = 0. \*\*\* $p \leq 0.001$ .

contents is not well understood [48], the presence of phagocytosed Pt within cochleae after years of implant use [15] implies that the majority of particulate Pt remained bound within macrophages in the cochlea.

Support for this hypothesis comes from the study of dermal macrophages associated with tattoo ink. While some ink particles are transported via the lymphatic system to the liver soon after injection [50], dermal macrophages capture and retain tattoo particles within the injection site. These macrophages provide an important scavenging and homeostatic

role in tissue but do not migrate [51, 52]. When tattoo pigment laden macrophages die, neighbouring macrophages recapture the released pigment ensuring the long-term persistence of tattoos [52].

### 4.3. Tissue response

The tissue response in the present study was in the form of a mature foreign body response that included a compact tissue capsule typically including a zone of macrophages around the electrode array, and a loose vascularized fibrous tissue response that occupied at least part of the scala tympani proximal to the electrode array. The extent of this tissue response was significantly greater in stimulated compared with implanted control cochleae. Moreover, there was little evidence of a tissue response within the scala tympani apical to the electrode array. These findings are consistent with our previous results in guinea pigs, and support the observation that electrical stimulation at high charge densities ( $>200 \mu\text{C cm}^{-2} \text{ phase}^{-1}$ ) evoke an increased tissue response [16, 17].

This stimulus-induced tissue response may be associated with the formation of electrochemical products at the electrode–tissue interface. We have previously shown that the extent of the response is not related to the degree of Pt corrosion [17]; however, other electrochemical reaction products may alter the electrolyte environment adjacent to the electrode, evoking the response. To this end, transient stimulus-induced changes in electrode impedance, that may be associated with an altered local electrochemical environment at the electrode–tissue interface, are commonly reported in a clinical setting [22]. Alternatively, the high electric fields present near the electrode results in the electroporation of cells, initiating an immune cascade [53, 54].

Finally, we previously described a focal region of necrotic tissue proximal to electrodes stimulated at charge densities  $\geq 267 \mu\text{C cm}^{-2} \text{ phase}^{-1}$  [16, 17].

**Table 2.** ICP-MS trace levels of Pt (ng/per mg half cochlea) for each stimulated and implanted unstimulated control cochlea and Pt (mg kg<sup>-1</sup>) from brain, liver and kidney.

Animal ID	Stimulated cochlea (ng/per mg half cochlea)	Control cochlea (ng/per mg half cochlea)	Brain (mg kg <sup>-1</sup> )	Liver (mg kg <sup>-1</sup> )	Kidney (mg kg <sup>-1</sup> )
HCD_1	1920	58	<0.01	<0.01	0.03
HCD_2	1300	87	<0.01	<0.01	0.01
HCD_3	3360	91	<0.01	<0.01	<0.01
HCD_4	360	20	<0.01	<0.01	<0.01
HCD_5	2249	165	<0.01	<0.01	<0.01
HCD_6	2090	220	<0.01	<0.01	<0.01
Combined	—	—	<0.01	<0.01	0.01

Note: There was sufficient brain, liver, and kidney tissue to perform two sets of measurements and also perform an analysis on tissue samples combined across all six animals. These results were highly reproducible and means are presented here. There was insufficient material to perform duplicate measurements on cochlear tissue.

There was no evidence of such a response in the present study, indicating that the necrotic response was sub-chronic and had resolved by 7 weeks of stimulation (HCD\_1; table 1).

#### 4.4. Impedances and electrical impedance spectroscopy

A number of centre-electrodes were excluded from use over the course of the stimulation program due to high common ground impedance recordings (>20 k $\Omega$ ). In the majority of cases, the high impedance was due to a tissue response rather than an open circuit as serial impedance recordings confirmed that the electrode was viable (<100 k $\Omega$ ). This was further supported by the EIS results, in which the high frequency (100 kHz) impedance magnitude, reflecting the resistance of the electrolyte and tissue adjacent to the electrode [6], was significantly higher over time for the electrodes on the stimulated array. Equivalent circuit analysis revealed significant changes in both the electrode and tissue components over the duration of the stimulation program. Supporting the large influence from the tissue response on the impedance, the values of  $K_t$  (analogous for a constant phase element to the capacitance of a pure capacitor) and  $\alpha_t$  (a measure of how capacitor-like ( $\alpha = 1$ ) or resistor-like ( $\alpha = 0$ ) the constant phase element is) [26, 27], significantly increased at 3 and 6 months post-implantation for electrodes on the stimulated array only. Both stimulated and control cochleae exhibited an increase in the resistive component of the tissue layer over time (indicated by  $\Delta R$  and  $R_\infty$ ), which is consistent with the histological finding that both cochleae exhibited a tissue response. However, the value of  $\Delta R$ , which dominates the total tissue resistance compared to  $R_\infty$ , was three times higher for the unstimulated control electrodes compared with the stimulated electrodes at the 6 month time point. This may indicate a delayed tissue response around the unstimulated control electrodes. There is evidence in humans for a tissue response starting at around 3 months and maturing around 6 months, particularly for less frequently stimulated electrodes [55].

The low frequency magnitude and phase of the EIS converge at 6 months, which is surprising, since the low frequency impedance is heavily influenced by the electrode/tissue interface rather than the surrounding tissue. Additionally, the electrode components of the impedance in the equivalent model exhibit similar behavior between unstimulated control and stimulated electrodes, with only a time effect on  $K_e$  and  $\alpha_e$ . Because the stimulated electrodes exhibited large amounts of corrosion, we would expect there to be large differences in the low frequency impedance of  $K_e$  and  $\alpha_e$  in stimulated compared to unstimulated control values. However, the results from the EIS and model parameters need to be interpreted with caution because the recordings at 6 months included fewer electrodes at the centre of the tripoles due to the drop-out rate of the electrodes.

Interestingly, the common ground impedances remained relatively consistent over time. The corrosion associated with the centre-electrodes may be expected to reduce electrode impedance. However, standard impedance was taken using a 25  $\mu$ s pulse and therefore somewhat equivalent to mid to high frequencies in the EIS spectrum. It is likely, therefore, that any reduction in impedance of the electrodes via corrosion was counteracted by the tissue response, resulting in an overall cancellation of these effects.

Correlations between the final common ground impedance with both tissue response and the electrode corrosion score were poor, while there was a moderate correlation between the tissue response and corrosion scores. Stimulated electrodes at the centre of the tripole exhibited more corrosion, and the stimulated cochlea had a greater tissue response. The poor correlations between the impedance, tissue response, and corrosion may reflect the limitations of the methodology in identifying the precise location of the tissue response relative to a specific electrode. Alternatively it may reflect a broad response.

#### 4.5. Cyclic voltammograms, CSC and CIL

The *in vivo* CVs presented here using bipolar and tripolar electrode configurations are likely to be

different from the ideal CVs measured for Pt in the laboratory (e.g. [6]) for several reasons:

- (a) unlike traditional CVs, our counter and reference electrodes (one or two intracochlear electrodes) were small and not referenced to tissue potential. This means that as potential was swept in the cathodic direction the working electrode became cathodic and the counter electrode became anodic. Therefore, the cathodic potential in our configuration actually measured a combination of cathodic and anodic processes. Differential roughening from corrosion of the working versus counter electrode and the fact that some measurements were in tripolar rather than bipolar configuration means there are likely to be some differences between anodic and cathodic sweeps. But as can be seen in figure 5(a), both cathodic and anodic sides of the sweep are very similar, particularly for the unstimulated control and 2 week stimulated cases where all electrodes were smooth.
- (b) both working and reference electrodes become polarised during the sweep. The potential is dropped across two electrodes, not one, so the potential between an individual electrode and tissue is about half what it would be in a traditional CV. So the  $-600$  mV and  $+800$  mV end points on our CVs actually represent potentials between individual electrodes and tissue of about  $-300$  mV and  $+400$  mV for bipolar configurations. For tripolar configurations the working electrode reaches a higher potential than for bipolar but still not the  $-600$  mV and  $+800$  mV in a traditional CV.
- (c) *in vitro* recorded CVs are typically recorded in oxygen and chlorine-free media as oxygen reduction and chlorine ion 'poisoning' of the Pt surface modify the CV. The *in vivo* environment contains abundant quantities of both, in addition to proteins.

It is difficult, therefore, to discern any features in the CV sweeps themselves, which are a complex mixture of anodic and cathodic process at potentials that do not relate to traditional CVs and are perhaps dominated by reactions such as oxygen reduction which are deliberately avoided in the laboratory. That being said, the magnitude of the current and charge passed, as measured by CSC, should still give a good measure of the real surface area or roughness factor of an electrode. This is because all surface reactions, anodic or cathodic and at whatever potential, increase proportionally with the real electrode area. In figure 5(b), the CSC, shows clear evidence of an increase in surface area (roughness) at the 3 and 6 month stimulated time points of about 60% compared to smooth control electrodes.

The CIL behaviour we observed was similar to that of the CSC discussed above, in that it increased for the stimulated electrodes at 3 and 6 months compared to the unstimulated controls and stimulated at 2 weeks. Like CV (and unlike EIS) this measure sweeps over a large potential range and is therefore likely to be independent of prior stimulation history. The ratio of the CIL at 6 months compared to the CIL at 2 weeks for stimulated electrodes is 1.6–1. Again, this would be consistent with a 60% increase in area of the stimulated electrodes due to electrochemical roughening. One difference in the case of CIL behaviour, however, is that there was a small and progressive increase in the CIL of the unstimulated control electrodes over time, with statistical difference between the 6 month and 2 week time points. In principle, the CIL value should reflect only the electrode/tissue interface and give a response proportional to the electrode area. While this method may work well in the laboratory, where the electrolyte is usually purely resistive, it may work less well in the *in vivo* environment where the 'electrolyte' is partly comprised of tissue.

#### 4.6. Status of the ANs

There were a number of reasons why ANs were selected as the most appropriate cell type to quantify when examining potential pathological effects of long-term stimulation and Pt corrosion products on the cochlea. First, ANs are the primary target neurons of cochlear implants. Secondly, ANs form the major group of excitatory cells within the cochlea and are therefore subject to potential adverse metabolic effects as well as local electrochemical changes, such as the generation of Pt ions and pH changes. Although there are subtle early markers indicating the onset of AN degeneration, once initiated, AN degeneration occurs quickly [56], making AN density a highly effective measure of AN loss. Finally, other excitatory tissue, particularly sensory hair cells, would be important to monitor in studies where there is residual hair cell survival; in the present study ototoxic drugs were used to remove hair cells prior to cochlear implantation in order to accurately model a profound hearing loss.

The present study has demonstrated that ANs do not undergo stimulus-induced degeneration using the stimulus parameters used in the present study. Furthermore, the significant levels of Pt corrosion product generated within the cochlea as a result of the stimulation showed no adverse effects on the AN population. Finally, the ECAP recordings showed that the chronically stimulated AN remained physiologically viable for the duration of the stimulus program. These responses exhibited no significant increase in threshold when compared with control cochleae, implying that there was no reduction in neural function as a result of chronic stimulation at these high charge densities.

It is important to note that a tripolar electrode configuration was used in the present study as it recruits relatively small numbers of ANs compared to monopolar stimulation [57], thereby allowing the use of high charge densities while maintaining comfortable loudness levels. It follows that using the same stimulus parameters, tripolar stimulation would not place the AN under the same level of metabolic stress as monopolar stimulation.

We previously reported a significant increase in the AN population proximal to the electrode array following stimulation for 28 d at 267 and 400  $\mu\text{C cm}^{-2}$  phase<sup>-1</sup> [16]. These results implied that there is a stimulus-induced rescue effect of ANs [56]; a result that has also been reported by others [18, 58]. In contrast to this earlier work, the present study, conducted over a 6 month period, showed no evidence of a stimulus-induced rescue effect of ANs. While depolarization of ANs via electrical stimulation may provide a trophic influence on ANs for short periods following deafness, our results show no evidence that a trophic influence is maintained over the long-term.

We did report a significant increase in AN survival in the apical region of the control versus chronically stimulated cochleae. We place little emphasis on this result as the apical region of the cochlea has limited tissue available for analysis, often resulting in large differences in AN density measurements.

#### 4.7. Clinical implications

The Shannon limit and the AAMI standard have been used to define safe stimulus limits for cochlear implants [7, 11]. We have demonstrated that long-term stimulation using stimulus parameters outside these limits does not damage ANs or the cochlea in general. At least for the stimulus parameters used in the present study, our results demonstrate that these standards provide a conservative measure of the limits of safe stimulation for cochlear implants. The conservative nature of the Shannon limit in assessing the threshold for tissue damage in neuromodulation devices has also been reported by others [10].

Although further studies are required to evaluate the safety of electrical stimulation of Pt electrodes at high charge densities in diverse anatomical locations, the ability to safely stimulate at charge densities above the AAMI standard [11] could expand the range of electrode arrays for clinical application for a variety of neural prostheses. This would include the use of smaller electrode contact areas in order to reduce the incidence of adverse off-target effects associated with electrical stimulation. It may be that such electrodes, if intended for long term use, will need materials that offer greater dissolution resistance than smooth Pt (e.g. [23]). Our study did not attempt to quantify the dissolution rate of the electrodes; however, it seems likely that electrode longevity rather than metabolic damage or cytotoxicity, will prove the limiting factor in the use of smooth Pt electrodes.

It is important to consider the clinical implications associated with the accumulation of Pt corrosion products both systemically and within the cochlea. Generally, Pt exposure in humans is typically associated with either environmental or clinical origins. Environmentally, the major source of Pt exposure is via ingestion of nanoparticles through the respiratory and digestive tract from automobile catalytic converters [59]. These particles accumulate in the liver, spleen, kidney, and lungs. Although toxicology appears dependent on particle size, there is currently insufficient data to define safe levels of exposure [59].

The major clinical source of Pt is associated with the use of Pt-based chemotherapy drugs such as cisplatin. Administered systemically, cisplatin accumulates and is retained within the cochlea for years [60, 61]; although the ratio of Pt bound within cisplatin versus free (unbound) Pt *in vivo* is unknown [62]. The degree of ototoxicity appears to be related to both the level and duration of its accumulation in the cochlea [63]. Experimental studies have demonstrated greater accumulation of Pt in liver, spleen, and kidney [61, 62], clearance from these organs is much more rapid [62]. At high doses cisplatin is nephrotoxic, although this is thought to be associated with the cellular mechanisms associated with cisplatin's effect on tumours rather than the toxicity of Pt *per se* [60]. Clinical studies have shown that Pt accumulated in the kidney is removed over time and is not correlated with a reduction in kidney function [64].

In addition to the presence of Pt debris associated with cochlear implant use, there is evidence of Pt corrosion associated with the long-term use of other neural prostheses. Post-mortem evaluation of Pt electrodes from a patient implanted with a cortical vision prosthesis for more than three decades revealed some degradation of Pt electrodes [42]. Although the extent of stimulation associated with this patient was unknown, the corrosion was not only associated with electrical stimulation; electrodes with little apparent stimulation history were thought to have undergone degradation as a result of long-term exposure to the biological environment [42]. In addition, electron dense particulate material has been reported in tissue samples taken from patients after long-term deep brain stimulation [65, 66]. In one study, multinucleated giant cells and macrophages containing electron-dense inclusions of presumably phagocytosed Pt was observed at the electrode-tissue interface [66].

Examples of non-Pt metallic corrosion contaminants are also described in the clinical literature; in particular wear and corrosion debris associated with metal-on-metal hip replacement. This is widely reported due to the large number of patients involved and the extent of the metallic debris generated; it is estimated that between  $10^{12}$  and  $10^{14}$  wear particles are produced annually from these devices [67]. Tissue

surrounding the implant is often discoloured and necrotic; and macrophages within this region contain metallic particles consistent with the alloy used in the implant [68]. In addition, extensive transportation of the metallic debris is also observed; while larger metallic particles remain in the vicinity of the implant, metal ions and nanoparticles are transported via the lymphatic system. Metal wear debris has been reported in the liver, spleen, and lymph nodes, while metal ions were detected in both blood and urine [67–69]. Despite the presence of extensive metallic contaminants, the adverse effects on the remote organs were regarded as insignificant [68, 69].

To place the present results in perspective, given that a Pt concentration of 10 and 30 parts per billion (w/w) was found in the kidneys of only two of six animals, and there was no evidence of Pt found elsewhere in any animal, systemic Pt toxicity due to electrode dissolution within the cochlea, even under extremely high charge density stimulation, would not appear to be of clinical significance.

#### 4.8. Limitations of the study

Although there was no evidence of any measurable adverse effects on cochlear tissue observed in the present study it is important to consider a number of limitations associated with this research. First, the study was limited to the use of six animals and one animal model. Second, the use of a single stimulation mode is not used clinically. Third, there is only one data point for histology so we cannot establish the longitudinal profile of Pt dissolution within the cochlea. Fourth, the present work did not determine the type or extent of the cochlear macrophage response. Fifth, it was not possible to provide a fully quantitative assessment of the dissolved Pt; we did not determine if Pt was excreted from the body or resided in organs that were not analysed. Finally, although this study examined changes occurring after periods of up to 6 months of stimulation, this duration only represents a fraction of expected period of clinical use.

## 5. Conclusions

Continuous electrical stimulation of Pt electrodes at a charge density of  $267 \mu\text{C cm}^{-2} \text{ phase}^{-1}$  using a tripolar electrode configuration over a period of 6 months did not result in a reduction in AN density or evoked-potential threshold associated with the stimulation despite a stimulus-induced tissue response and the presence of Pt corrosion product within the cochlea. The tissue response was significantly greater in the stimulated versus implanted unstimulated control cochleae, and stimulated electrodes exhibited significantly more corrosion compared with unstimulated electrodes. Increased CSC and CIL observed in chronically stimulated electrodes

reflected the more extensive electrode corrosion. Notably, Pt corrosion was also clearly evident in implanted unstimulated control cochleae, although the levels were significantly less than stimulated cochleae. The majority of Pt remains within the cochlea; only two of the six animals in the study showed just detectable levels of Pt in kidney tissue, while liver and brain showed no evidence of Pt. The level of systemic Pt does not appear to be of clinical significance.

Our research also demonstrated that the dissolution of Pt electrodes within the cochlea, did not result in the widespread migration of Pt corrosion products systemically; the great majority of particulate Pt was phagocytosed and remained bound within macrophages of the cochlea. Finally, electrode longevity rather than tissue damage is likely to prove the limiting factor in the use of Pt electrodes at high charge densities. Neural stimulation well above the typical charge densities currently used clinically, would benefit from the use of more electrochemically stable electrode materials. The development of such materials is clearly warranted.

## Acknowledgments

This work was supported by NIDCD (R01DC015031) and Cochlear Ltd The Bionics Institute acknowledges support of the Victorian Government through Operational Infrastructure Support Program. We thank E Trang, C Singleton, C McGowan, H Feng, J Zhou, N Critch, C Grenness, C Sloan, D Tuari, and S Barone from the Bionics Institute, and R Curtain from the SEM Facility at Bio21, University of Melbourne for their excellent technical assistance; staff at the National Measurement Institute of the Australian Government for ICP-MS analysis; Dr Karin Jandeleit-Dahm for advice on kidney function, and Dr Keiko Hirose and Dr Marlan Hansen for advice on macrophage longevity.

## ORCID iDs

Robert K Shepherd  <https://orcid.org/0000-0002-4239-3362>

Paul M Carter  <https://orcid.org/0000-0001-9286-1630>

Ashley N Dalrymple  <https://orcid.org/0000-0001-8566-7178>

Ya Lang Enke  <https://orcid.org/0000-0002-0124-7481>

Andrew K Wise  <https://orcid.org/0000-0001-9715-8784>

Alex Thompson  <https://orcid.org/0000-0002-8012-872X>

James B Fallon  <https://orcid.org/0000-0003-2686-3886>

## References

- [1] Cogan S F, Ludwig K A, Welle C G and Takmakov P 2016 Tissue damage thresholds during therapeutic electrical stimulation *J. Neural Eng.* **13** 021001
- [2] Merrill D R, Bikson M and Jefferys J G 2005 Electrical stimulation of excitable tissue: design of efficacious and safe protocols *J. Neurosci. Methods* **141** 171–98
- [3] Brummer S B and Turner M J 1977 Electrochemical considerations for safe electrical stimulation of the nervous system with platinum electrodes *IEEE Trans. Biomed. Eng.* **24** 59–63
- [4] Black R C and Hannaker P 1980 Dissolution of smooth platinum electrodes in biological fluids *Appl. Neurophysiol.* **42** 366–74
- [5] Huang C Q, Carter P M and Shepherd R K 2001 Stimulus induced pH changes in cochlear implants: an *in vitro* and *in vivo* study *Ann. Biomed. Eng.* **29** 791–802
- [6] Cogan S F 2008 Neural stimulation and recording electrodes *Annu. Rev. Biomed. Eng.* **10** 275–309
- [7] Shannon R V 1992 A model of safe levels for electrical stimulation *IEEE Trans. Biomed. Eng.* **39** 424–6
- [8] McCreery D B, Agnew W F, Yuen T G and Bullara L 1990 Charge density and charge per phase as cofactors in neural injury induced by electrical stimulation *IEEE Trans. Biomed. Eng.* **37** 996–1001
- [9] Shepherd R K, Villalobos J, Burns O and Nayagam D A X 2018 The development of neural stimulators: a review of preclinical safety and efficacy studies *J. Neural Eng.* **15** 041004
- [10] Kumsa D et al 2018 Public regulatory databases as a source of insight for neuromodulation devices stimulation parameters *Neuromodulation* **21** 117–25
- [11] ANSI 2017 Cochlear implant systems: requirements for safety, functional verification, labeling and reliability reporting ANSI/AAMI CI86:2017 (Arlington, VA: AAMI) p 169
- [12] Clark G M et al 2014 Biomedical studies on temporal bones of the first multi-channel cochlear implant patient at the university of Melbourne *Cochlear Implants Int.* **15** S1–15
- [13] Spiers K, Cardamone T, Furness J B, Clark J C M, Patrick J F and Clark G M 2016 An x-ray fluorescence microscopic analysis of the tissue surrounding the multi-channel cochlear implant electrode array *Cochlear Implants Int.* **17** 129–31
- [14] Nadol J B Jr, O'Malley J T, Burgess B J and Galler D 2014 Cellular immunologic responses to cochlear implantation in the human *Hear. Res.* **318** 11–17
- [15] O'Malley J T, Burgess B J, Galler D and Nadol J B Jr 2017 Foreign body response to silicone in cochlear implant electrodes in the human *Otology Neurotology* **38** 970–7
- [16] Shepherd R K, Carter P M, Enke Y L, Wise A K and Fallon J B 2019 Chronic intracochlear electrical stimulation at high charge densities results in platinum dissolution but not neural loss or functional changes *in vivo* *J. Neural Eng.* **16** 026009
- [17] Shepherd R K et al 2020 Chronic intracochlear electrical stimulation at high charge densities: reducing platinum dissolution *J. Neural Eng.* **17** 056009
- [18] Leake P A, Hradek G T and Snyder R L 1999 Chronic electrical stimulation by a cochlear implant promotes survival of spiral ganglion neurons after neonatal deafness *J. Comp. Neurol.* **412** 543–62
- [19] Fallon J B, Irvine D R and Shepherd R K 2009 Cochlear implant use following neonatal deafness influences the cochleotopic organization of the primary auditory cortex in cats *J. Comp. Neurol.* **512** 101–14
- [20] Shepherd R, Verhoeven K, Xu J, Risi F, Fallon J and Wise A 2011 An improved cochlear implant electrode array for use in experimental studies *Hear. Res.* **277** 20–27
- [21] Shepherd R K, Wise A K, Enke Y L, Carter P M and Fallon J B 2017 Evaluation of focused multipolar stimulation for cochlear implants: a preclinical safety study *J. Neural Eng.* **14** 046020
- [22] Newbold C, Mergen S, Richardson R, Seligman P, Millard R, Cowan R and Shepherd R 2014 Impedance changes in chronically implanted and stimulated cochlear implant electrodes *Cochlear Implants Int.* **15** 191–9
- [23] Dalrymple A N, Robles U A, Huynh M, Nayagam B A, Green R A, Poole-Warren L A, Fallon J B and Shepherd R K 2020 Electrochemical and biological performance of chronically stimulated conductive hydrogel electrodes *J. Neural Eng.* **17** 026018
- [24] McAdams E T and Jossinet J 1995 Tissue impedance: a historical overview *Physiol. Meas.* **16** A1–13
- [25] Lempka S F, Miocinovic S, Johnson M D, Vitek J L and McIntyre C C 2009 *In vivo* impedance spectroscopy of deep brain stimulation electrodes *J. Neural Eng.* **6** 046001
- [26] Macdonald J R 1987 *Impedance Spectroscopy* (New York: Wiley)
- [27] Grimnes S and Martinsen O G 2000 *Bioimpedance and Bioelectricity Basics* (New York: Academic)
- [28] Leung R T, Shivdasani M N, Nayagam D A and Shepherd R K 2015 *In vivo* and *in vitro* comparison of the charge injection capacity of platinum macroelectrodes *IEEE Trans. Biomed. Eng.* **62** 849–57
- [29] Senn P 2015 Neurostimulation for the management of pain PhD University of Melbourne, Melbourne
- [30] Patrick J F, Seligman P M, Money D K and Kuzma J A 1990 Engineering *Cochlear Prosthesis* ed G M Clark, Y C Tong and J F Patrick (Edinburgh: Churchill Livingstone) pp 99–124
- [31] Wise A K, Tan J, Wang Y, Caruso F and Shepherd R K 2016 Improved auditory nerve survival with nanoengineered supraparticles for neurotrophin delivery into the deafened cochlea *PLoS One* **11** e0164867
- [32] Dalrymple A N et al 2019 Electrochemical and mechanical performance of reduced graphene oxide, conductive hydrogel, and electrodeposited Pt-Ir coated electrodes: an active *in vitro* study *J. Neural Eng.* **17** 016015
- [33] Topalov A A, Cherevko S, Zeradjanin A R, Meier J C, Katsounaros I and Mayrhofer K J J 2014 Towards a comprehensive understanding of platinum dissolution in acidic media *Chem. Soc.* **5** 631–8
- [34] Noel J-M, Yu Y and Mirkin M V 2013 Dissolution of Pt at moderately negative potentials during oxygen reduction in water and organic media *Langmuir* **29** 1346–50
- [35] Percival S J, Dick J E and Bard A J 2017 Cathodically dissolved platinum resulting from the O<sub>2</sub> and H<sub>2</sub>O<sub>2</sub> reduction reactions on platinum ultramicroelectrodes *Anal. Chem.* **89** 3087–92
- [36] Untereker D F and Bruckenstein S 1974 A dissolution redeposition mechanism for roughening of platinum electrodes by cyclic potential programs *J. Electrochem. Soc.* **121** 360–2
- [37] Azaroual M, Romand B, Freyssinet P and Disnar J-R 2001 Solubility of platinum in aqueous solutions at 25°C and pHs 4–10 under oxidizing conditions *Geochim. Cosmochim. Acta* **65** 4453–66
- [38] Ballestrasse C L, Ruggeri R T and Beck T R 1985 Calculations of the pH changes produced in body tissue by a spherical stimulation electrode *Ann. Biomed. Eng.* **13** 405–24
- [39] Agnew W F, Yuen T G, McCreery D B and Bullara L A 1986 Histopathologic evaluation of prolonged intracortical electrical stimulation *Exp. Neurol.* **92** 162–85
- [40] Robblee L S, McHardy J, Agnew W F and Bullara L A 1983 Electrical stimulation with Pt electrodes. VII. Dissolution of Pt electrodes during electrical stimulation of the cat cerebral cortex *J. Neurosci. Methods* **9** 301–8
- [41] Barrese J C, Aceros J and Donoghue J P 2016 Scanning electron microscopy of chronically implanted intracortical microelectrode arrays in non-human primates *J. Neural Eng.* **13** 026003
- [42] Towle V L, Pytel P, Lane F, Plass J, Frim D M and Troyk P R 2020 Postmortem investigation of a human cortical visual prosthesis that was implanted for 36 years *J. Neural Eng.* **17** 045010

- [43] Cochlear 2020 CochlearTM nucleus CI632 cochlear implant with slim modiolar electrode physician's guide (available at: [www.cochlear.com](http://www.cochlear.com))
- [44] MedEl 2020 Mi1250 synchrony 2 surgical guide (available at: [www.medel.com](http://www.medel.com))
- [45] AdvancedBionics 2020 Surgeon's manual for the HiResTM ultra 3D (available at: [www.advancedbionics.com](http://www.advancedbionics.com))
- [46] Henle C, Meier W, Schuettler M, Boretius T and Stieglitz T 2009 Electrical characterisation of platinum, stainless steel and platinum/iridium as electrode materials for a new neural interface *IFMBE Proc.* vol 25 pp 101–3
- [47] Ganske G, Slavchevaab E, Van Ooyena A, Mokwaa W and Schnakenberga U 2011 Sputtered platinum–iridium layers as electrode material for functional electrostimulation *Thin Solid Films* **519** 3965–70
- [48] Levin R, Grinstein S and Canton J 2016 The life cycle of phagosomes: formation, maturation, and resolution *Immunol. Rev.* **273** 156–79
- [49] Botelho R J and Grinstein S 2011 Phagocytosis *Curr. Biol.* **21** R533–8
- [50] Sepehri M, Sejersen T, Qvortrup K, Lerche C M and Serup J 2017 Tattoo pigments are observed in the kupffer cells of the liver indicating blood-borne distribution of tattoo ink *Dermatology* **233** 86–93
- [51] Tamoutounour S et al 2013 Origins and functional specialization of macrophages and of conventional and monocyte-derived dendritic cells in mouse skin *Immunity* **39** 925–38
- [52] Baranska A et al 2018 Unveiling skin macrophage dynamics explains both tattoo persistence and strenuous removal *J. Exp. Med.* **215** 1115–33
- [53] Newbold C, Richardson R, Millard R, Seligman P, Cowan R and Shepherd R 2011 Electrical stimulation causes rapid changes in electrode impedance of cell-covered electrodes *J. Neural Eng.* **8** 036029
- [54] Newbold C, Richardson R, Millard R, Huang C, Milojevic D, Shepherd R and Cowan R 2010 Changes in biphasic electrode impedance with protein adsorption and cell growth *J. Neural Eng.* **7** 056011
- [55] Briggs R, O'Leary S, Birman C, Plant K, English R, Dawson P, Risi F, Gavrilis J, Needham K and Cowan R 2020 Comparison of electrode impedance measures between a dexamethasone-eluting and standard Cochlear™ Contour Advance® electrode in adult cochlear implant recipients *Hear. Res.* **390** 107924
- [56] Wise A K, Pujol R, Landry T G, Fallon J B and Shepherd R K 2017 Structural and ultrastructural changes to type I spiral ganglion neurons and schwann cells in the deafened guinea pig cochlea *J. Assoc. Res. Otolaryngol.* **18** 751–69
- [57] George S S, Wise A K, Shivdasani M N, Shepherd R K and Fallon J B 2014 Evaluation of focused multipolar stimulation for cochlear implants in acutely deafened cats *J. Neural Eng.* **11** 065003
- [58] Kanzaki S, Stover T, Kawamoto K, Prieskorn D M, Altschuler R A, Miller J M and Raphael Y 2002 Glial cell line-derived neurotrophic factor and chronic electrical stimulation prevent VIII cranial nerve degeneration following denervation *J. Comp. Neurol.* **454** 350–60
- [59] Czubacka E and Czerczak S 2019 Are platinum nanoparticles safe to human health? *Med. Pr.* **70** 487–95
- [60] Miller R P, Tadagavadi R K, Ramesh G and Reeves W B 2010 Mechanisms of Cisplatin nephrotoxicity *Toxins* **2** 2490–518
- [61] Madias N E and Harrington J T 1978 Platinum nephrotoxicity *Am. J. Med.* **65** 307–14
- [62] Breglio A M, Rusheen A E, Shide E D, Fernandez K A, Spielbauer K K, McLachlin K M, Hall M D, Amable L and Cunningham L L 2017 Cisplatin is retained in the cochlea indefinitely following chemotherapy *Nat. Commun.* **8** 1654
- [63] Gersten B K, Fitzgerald T S, Fernandez K A and Cunningham L L 2020 Ototoxicity and platinum uptake following cyclic administration of platinum-based chemotherapeutic agents *J. Assoc. Res. Otolaryngol.* **21** 303–21
- [64] Uozumi J, Ueda T, Yasumasu T, Koikawa Y, Naito S, Kumazawa J, Kamura T, Nakano H and Sueishi K 1993 Platinum accumulation in the kidney and changes in creatinine clearance following chemotherapy with cisplatin in humans *Urol. Int.* **51** 57–61
- [65] Haberler C, Alesch F, Mazal P R, Pilz P, Jellinger K, Pinter M M, Hainfellner J A and Budka H 2000 No tissue damage by chronic deep brain stimulation in Parkinson's disease *Ann. Neurol.* **48** 372–6
- [66] Moss J, Ryder T, Aziz T Z, Graeber M B and Bain P G 2004 Electron microscopy of tissue adherent to explanted electrodes in dystonia and Parkinson's disease *Brain* **127** 2755–63
- [67] Doorn P F, Campbell P A, Worrall J, Benya P D, McKellop H A and Amstutz H C 1998 Metal wear particle characterization from metal on metal total hip replacements: transmission electron microscopy study of periprosthetic tissues and isolated particles *J. Biomed. Mater. Res.* **42** 103–11
- [68] Liao Y F, Hoffman E, Wimmer M, Fischer A, Jacobs J and Marks L 2013 CoCrMo metal-on-metal hip replacements *Phys. Chem. Chem. Phys.* **15** 746–56
- [69] Urban R M, Jacobs J J, Tomlinson M J, Gavrilovic J, Black J and Peoc'h M 2000 Dissemination of wear particles to the liver, spleen, and abdominal lymph nodes of patients with hip or knee replacement *J. Bone Joint Surg. Am.* **82** 457–76